

Water alignment, dipolar interactions, and multiple proton occupancy during water-wire proton transport

Tom Chou

Dept. of Biomathematics and IPAM, Los Angeles, CA 90095-1766

(Dated: November 2, 2018)

A discrete multistate kinetic model for water-wire proton transport is constructed and analyzed using Monte-Carlo simulations. The model allows for each water molecule to be in one of three states: oxygen lone pairs pointing leftward, pointing rightward, or protonated (H_3O^+). Specific rules for transitions among these states are defined as protons hop across successive water oxygens. We then extend the model to include water-channel interactions that preferentially align the water dipoles, nearest-neighbor dipolar coupling interactions, and coulombic repulsion. Extensive Monte-Carlo simulations were performed and the observed qualitative physical behaviors discussed. We find the parameters that allow the model to exhibit superlinear and sublinear current-voltage relationships and show why alignment fields, whether generated by interactions with the pore interior or by membrane potentials *always* decrease the proton current. The simulations also reveal a “lubrication” mechanism that suppresses water dipole interactions when the channel is multiply occupied by protons. This effect can account for an observed sublinear-to-superlinear transition in the current-voltage relationship.

Keywords: proton transport, asymmetric exclusion process, water wire

INTRODUCTION

The transport of protons in aqueous media and across membranes is a fundamental process in chemical reactions, solvation, and pH regulation in cellular environments [Alberts *et al.* 1994, Grabe & Oster 2001]. Proton transport in confined geometries is also relevant for ATP synthesis [Boyer 1997] and light transduction by bacteriorhodopsin [Lanyi 1995]. In this paper, we develop a lattice model for describing proton transport in *one-dimensional* environments. This study is motivated by numerous measurements of proton conduction across channels embedded in lipid membranes [Akeson & Deamer 1991, Busath *et al.* 1998, Cotten *et al.* 1999, Cukierman 1997, Deamer 1987, Eisenman *et al.* 1980]. Experiments are typically performed using membrane-spanning gramicidin channels that are only a few Angstroms in diameter. This geometric constraint imposes a single-file structure on the configurations of the interior water molecules [Hille & Schwarz 1978, Hladky & Haydon 1972].

Under the same electrochemical potential gradients, conduction of protons across ion channels occurs at a rate typically an order of magnitude higher than that of other small ions. This supports a “water-wire” mechanism [Akeson & Deamer 1991, Nagle & Horowitz 1978, Nagle & Tristan-Nagle 1983, Nagle 1987], first proposed by Grotthuss [Agmon 1995, Grotthuss 1806]. Across a water-wire, protons are shuttled across lone pairs of water oxygens as they successively protonate the waters along the single-file chain. However, since the hydrogens are indistinguishable, any one of the hydrogens in a water cluster (*e.g.*, any of the three hydrogens on a hydronium) can hop forward along the chain to protonate the next water molecule or cluster of water molecules (*cf.* Fig. 1). This mechanism naturally allows much faster overall con-

duction of protons compared to other small ions which have to wait for the entire chain of water molecules ahead of it to fluctuate across the pore in order to traverse the channel.

A peculiar feature of measured current-voltage relationships is a crossover from sublinear to superlinear behavior as the pH of the reservoirs is lowered. Measurements by Eisenman [Eisenman *et al.* 1980] were carried out in symmetric solutions in the 1-3 pH range, and the results were recently reproduced by Busath *et al.* [Busath *et al.* 1998] and Rokitskaya *et al.* [Rokitskaya *et al.* 2002]. These experiments were performed using simple, relatively featureless gramicidin A (gA) channels. One leading hypothesis is that the nonlinear proton current-voltage relationships arise from the intrinsic proton dynamics within such simple channels. Specifically, multiple proton occupancy and repulsion among protons within the channel may give rise to the observed nonlinearity [Hille & Schwarz 1978, Phillips *et al.* 1999, Schumaker *et al.* 2001].

There have been a number of recent theoretical studies of water-wire proton conduction. Extensive simulations on the quantum dynamics of proton exchange in essentially small, representative water clusters in vacuum have been used to predict microscopic hopping rates between water clusters [Bala *et al.* 1994, Sadgeghi & Cheng 1999, Marx *et al.* 1999, Mavri & Berendsen 1995, Mei *et al.* 1998, Sagnella *et al.* 1996, Schmitt & Voth 1999]. Pomès and Roux [Pomès & Roux 1996] have performed classical molecular dynamics (MD) simulations on water-channel interactions, proton hopping, and water reorientation. They derive effective potentials of mean force describing the energy barriers encountered by a single proton within the pore. Since MD simulations are presently limited to only processes that occur over a few nanoseconds, none of these computational methods are efficient at probing very long time, steady-state transport behavior. On

a more macroscopic, phenomenological level, Sagnella *et al.* [Sagnella & Voth 1996] and Schumaker *et al.* [Schumaker *et al.* 2000, Schumaker *et al.* 2001] have considered the long-time behavior of a single proton and dipole "defect" diffusing in a single-file channel. The parameters used in these studies, including effective energy profiles and kinetic rates, were derived from MD simulations. Although the basic underlying structure assumed by all of these transport models qualitatively resembles the Grotthuss mechanism, they have not addressed multiple proton occupancy.

In this paper, we will explore the intrinsically non-linear proton dynamics along a single-file water-wire. We use a dynamical lattice model that defines the discrete structural states of the water-wire that approximate the continuous molecular orientations. Although the lattice model provides a different approach from MD simulations, it is more amenable to analysis at longer time scales, yet is connected to the microphysics inherent in MD simulations provided a consistent correspondence between the parameters is made. Rather than enumerating all possible molecular configurations, our lattice approach resembles that developed for molecular motors [Fisher & Kolomeisky 1999], mRNA translation [MacDonald & Gibbs 1969, Chou 2003], traffic flow [Karimipour 1999, Schreckenberg *et al.* 1995], and ion and water transport in single-file channels [Chou 1998, Chou 1999, Chou & Lohse 1999]. Here, the proton occupancy along the water-wire will be self-consistently determined by the prescribed lattice dynamics. The parameters used in our model are transition rates among discrete states that in principle can be independently computed from relatively short-time MD simulations. Despite the approximations inherent in our discrete model, it qualitatively treats the effects of proton-proton repulsion and water-water dipole interactions.

MODEL AND METHODS

Qualitatively, protons hop from oxygen to oxygen during transport. The successive hops clearly do not have to involve an individually tagged proton; in this respect, proton currents resemble electrical conduction in a conductor. Many measurements of proton conduction across membranes are performed on the gramicidin model system. The interior diameter of gramicidin A (gA) is $\sim 3-4$ Angstroms and can only accommodate water in a single file chain. Although the number of water molecules in this chain is a fluctuating quantity, their dynamics in and out of the channel will be assumed to be much slower than that of their orientational rearrangements and proton hopping [Hummer *et al.* 2001, Kalra *et al.* 2003]. We can thus treat the water wire as containing a fixed, average number of water molecules. Within typical transmembrane channels, are $N \approx 8 - 26$ single-file waters [Levitt *et al.* 1978, Wu & Voth 2003].

Figure 1A shows a schematic of our model. We first assume that each "site" along the pore is occupied by a single oxygen atom which may either be

part of neutral water, H_2O , or a hydronium (H_3O^+) ion. Although protonated oxygens in bulk are often associated with larger complexes such as H_5O_2^+ (Zundel cation), or H_9O_4^+ (Eigen cation), in confined geometries, the formation of the larger complexes is suppressed [Lynden-Bell & Rasaiah 1996]. Furthermore, we will show that our discrete model depicted in Fig. 1A can incorporate the dynamics of reactive proton transfer among transient clusters by an appropriate redefinition of a lattice site to contain the entire cluster.

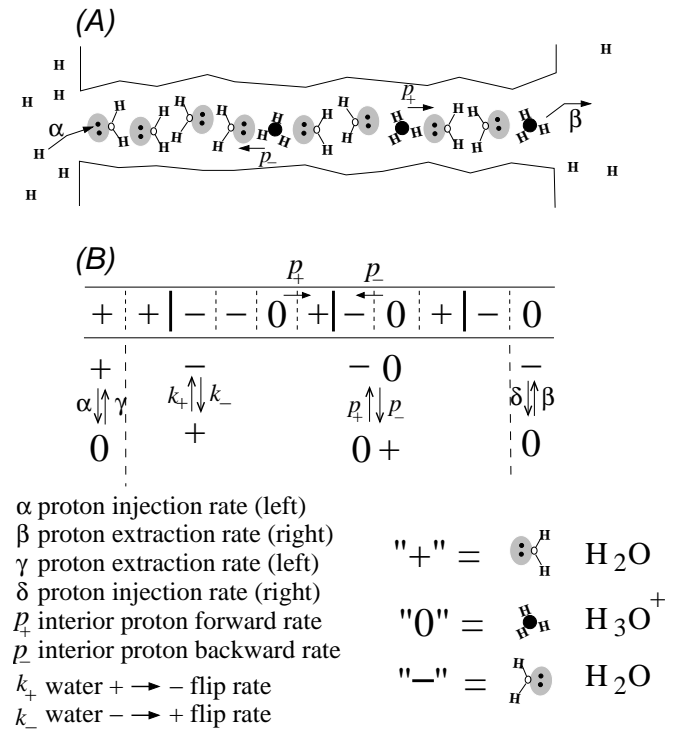


FIG. 1: (A) Schematic of an $N = 11$, three-species exclusion model that captures the steps in a Grotthuss mechanism of proton transport along a water wire. For typical ion channels that span lipid membranes, $N \sim 10-20$. The transition rates are labeled in (B) and in the legend. Water dipole kinks are denoted by thick lines.

Neutral waters have permanent dipole moments and electron lone-pair orientations that can rotate thermally. For simplicity, we bin all water dipoles (hydrogens) that point towards the right as "+" particles, while those pointing more or less to the left are denoted "-" particles. The singly protonated species H_3O^+ is hybridized to a nearly planar molecule. Therefore, we will assume that hydronium ions are symmetric with respect to transferring a proton forward or backwards, provided the adjacent waters are in the proper orientation and there are no external driving forces (electric fields). Each lattice site can exist in only one of three states: 0, +, or -, corresponding to protonated, right, or left states, respectively. Labeling the occupancy configurations $\sigma_i = \{-1, 0, +1\}$, allows for fast integer computation in simulations.

In addition to proton exclusion, the transition rules are constrained by the orientation of the waters at each site and are defined in Fig. 1B. A proton can enter the first site ($i = 1$) from the left reservoir and protonate the first water molecule with rate α only if the hydrogens of the first water are pointing to the right (such that its lone-pair electrons are left-pointing, ready to accept a proton). Conversely, if a proton exits from the first site back into the left reservoir (with rate γ), it leaves the remaining hydrogens right-pointing. In the pore interiors, a proton at site i can hop to the right(left) with rate $p_+(p_-)$ only if the adjacent particle is a right(left)-pointing, unprotonated water molecule. If such a transition is made, the water molecule left at site i will be left(right) pointing. Physically, as a proton moves to the right, it leaves a wake of $-$ particles to its left. A left moving proton leaves a trail of $+$ particles to its right. These trails of $-$ or $+$ particles are unable to accept another proton from the same direction. Protons can follow each other successively only if water molecules can reorient such that these trails of $+$'s or $-$'s are thermally washed out. Water reorientation rates are denoted k_{\pm} (cf. Figs. 1B and 2). Protons at the rightmost end of the water wire (at site $i = N$), exit with rate β , which is different from p_+ since the local microenvironment (*e.g.*, typical distance to acceptor electrons) of the bulk waters that accept this last proton is different from that in the pore interior. From the right reservoir, protons can hop back into the water wire with rate δ if a water in the “ $-$ ” configuration is at site $i = N$. The entrance rates α and δ are functions of at least the proton concentration in the respective reservoirs. Figure 2 shows a representative time series of the evolution of a specific configuration. The rate-limiting steps in steady-state proton transfer across biological water channels are thought to be associated with water flipping [Pomès & Roux 1998].

The lattice discretization for individual H_3O^+ ions need not be interpreted literally. Larger complexes can be effectively modeled by reinterpreting p_{\pm}, k_{\pm} , and the basic unit of hopping for the proton. For example, if certain conditions obtain, where ions are predominantly two-oxygen clusters (H_5O_2^+), we defined each pair of waters as occupying a single lattice site, k_{\pm} as an effective reorientation time for the following pair of waters, and p_{\pm} as the hopping rate to an adjacent oxygen lone-pair. The Grotthuss water-wire mechanism is qualitatively preserved as long as the proper identification with the microphysics is made.

All eight “parameters” used in our model (the rates $p_{\pm}, k_{\pm}, \alpha, \beta, \gamma, \delta$), can be related to measured bulk quantities or derived from short-time MD simulations. They are a minimal set and are equivalent to the numerous bulk parameters used in other models [Schumaker *et al.* 2001], such as the bulk proton diffusion constant, water orientational diffusion constants, etc. Using similar MD approaches then, one should be able to approximately fix the parameters used in our model. For example, variations in the potential of mean

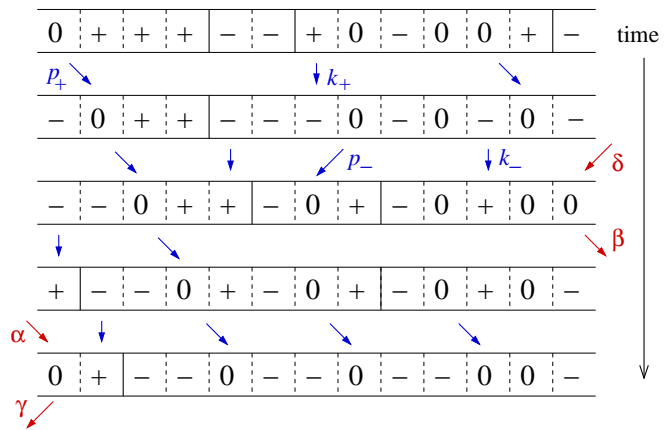


FIG. 2: A time series depicting a number of representative transitions obeying the dynamical constraints of our model. A proton (0) at site i can move to the right with rate p_+ only if site $i + 1$ is occupied by a properly aligned (lone-pair electrons pointing to the left) water molecule (+). When a proton leaves site i to the right, it leaves behind a water in state “ $-$ ”, with lone pair electrons pointing to the right. Protons at site i can also move to the left with rate p_- if site $i - 1$ is a water in the “ $-$ ” state. In this case, a water is left behind at behind site i in the “ $+$ ” state. The neutral water molecules must flip ($+$ \leftrightarrow $-$) in order for a nonzero steady-state current to exist.

- (A) $\dots 00+0\dots \longrightarrow \dots 0-00\dots \quad \Delta E=H-V$
 (B) $\dots 00+-\dots \longrightarrow \dots 0-0-\dots \quad \Delta E=H-K-R-V$
 (C) $\dots +++\dots \longrightarrow \dots +-+\dots \quad \Delta E=H+2K$
 (D) $\dots 00++\dots \longrightarrow \dots 0-0+\dots \quad \Delta E=H+K-R-V$

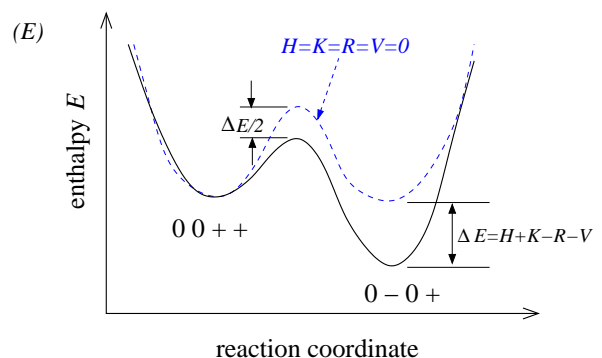


FIG. 3: (A – D) Energy differences between final and initial states which involve a change in ferroelectric coupling, net dipole moment, and repulsive interactions. (E) A representative energy barrier profile for $H = K = R = V = 0$ (dashed curves). The energy profile for $H, K, R, V \neq 0$ for a transition between the states considered in (D) is shown by the thick solid curve.

force along the pore (resulting from interactions of the different species with the constituents of the pore interior) are embodied by site-dependent transition rates p_{\pm} and k_{\pm} . Thus, MD-derived potentials of mean force used in previous models can also be implemented within our lattice framework. Such effects of local inhomogeneities in the hopping rates have been studied analytically and with MC simulations in related models [Kolomeisky 1998].

The basic model described above has been studied analytically in certain limits where exact asymptotic results for the steady-state proton current J were derived [Chou 2002]. However, this study did not explicitly include any interactions other than proton exclusion and proton transfer onto properly aligned water dipoles. Effects arising from forces such as repulsion between protons in close proximity, interactions between water dipoles and external electric fields, and dipolar coupling between neighboring waters need to be considered.

In Fig 3A, a proton moves down the electric potential reducing the total enthalpy by V , and a right-pointing dipole is converted into a left-pointing dipole at an energy cost of H . Since both initial and final states have adjacent, repelling protons, the repulsion energy R does not enter in the overall energy change. In Fig. 3B, a proton moves down the potential ($-V$), a “+” water is converted to a “-”, ($+H$), a dipole “domain wall” is removed ($-K$), and the repulsive energy between adjacent charged protons is relieved ($-R$). The representation of these nearest neighbor effects can be succinctly written in terms of the energy of a specific configuration

$$E[\{\sigma_i\}] = -K \sum_{i=1}^{N-1} \sigma_i \sigma_{i+1} - H \sum_{i=1}^N \sigma_i + R \sum_{i=1}^{N-1} (1 - \sigma_i^2)(1 - \sigma_{i+1}^2) - V \sum_{i=1}^N i(1 - \sigma_i^2). \quad (1)$$

The H, K, R, V parameters used in $E[\{\sigma_i\}]$ are all in units of $k_B T$ and represent

- H : energy cost for orienting a water dipole against external field
- K : energy cost for two oppositely oriented, adjacent dipoles
- R : repulsive Coulombic energy of two adjacent protons
- V : energy for moving a charged proton one lattice site against an external field.

V as the change in potential that a proton incurs as it moves between adjacent waters. The total transmembrane potential $V_{membrane} = NV$. The local dielectric environment across a channel can induce a spatially varying effective potential $V_{1 \leq i \leq N}$ [Edwards *et al.* 2002, Jordan 1984, Partenskii & Jordan 1992, Szygnow & von Kitzing 1999]. In this study, we

neglect this variation and assume constant V across the lattice.

In order to connect the quantities $H, K, R,$ and V to the rates $\alpha, \beta, \gamma, \delta, p_{\pm}, k_{\pm}$, we will assume the transitions occur over thermal barriers. Although barriers to proton hopping may be small, we employ the Arrhenius forms in order to obtain a simple relationship so that qualitative aspects of the effects of $H, K, R,$ and V can be illustrated. Activation-energy-based treatments for conduction across gramicidin channels have been previously studied [Chernyshev & Cukierman 2002]. When the more complicated interactions and external potentials are turned on, the effective transition rates $\xi \equiv \{\alpha, \beta, \gamma, \delta, p_{\pm}, k_{\pm}\}$ on which we base our Metropolis Monte-Carlo become

$$\xi = \xi_0 \exp\left(\frac{\Delta E}{2}\right), \quad (2)$$

where $\xi_0 \equiv \{\alpha_0, \beta_0, \gamma_0, \delta_0, p_0, k_0\}$ are rate prefactors when H, K, R, V and ΔE are zero. In defining Eq. 2, we have assumed that the energy barrier due to the difference $\Delta E = E[\{\sigma'_i\}] - E[\{\sigma_i\}]$ ($\{\sigma'_i\}$ and $\{\sigma_i\}$ are the final and initial state configurations, respectively) is evenly split between the barrier energies in the forward and backward directions. We use the convention that $p_+ = p_- = p_0$ and $k_+ = k_- = k_0$ when $V = 0$ and $H = 0$, respectively. The constraints and the state-dependent transition rates determined by Eqs. 1 and 2 completely define a nonequilibrium dynamical model which we study using MC simulations. Note that in the original model (Fig. 2) we *do not* assume transition barriers, but rather only that the dynamics are Markovian.

We first gained insight into the dynamics by considering numerical solutions to the full Master equation for a short three site ($N = 3$) channel. If we explicitly enumerated all $27 = 3^3$ states of the three site model, the Master equation for the 27 component state vector \vec{P} is

$$\frac{d\vec{P}(t)}{dt} = \mathbf{M}\vec{P}(t), \quad (3)$$

where \mathbf{M} is the transition matrix constructed from the rates ξ . In steady-state, the P_i are solved by inverting \mathbf{M} with the constraint $\sum_{i=1}^{27} P_i = 1$. The steady-state currents are found from the appropriate elements in P_i times the proper rate constants in the model. For example, if the probability that the three-site chain is in the configuration $(+ - 0)$ is denoted P_{12} , then the transition rate to state $P_{13} \equiv (+ - -)$ (corresponding to the ejection of a proton from the last site into the right reservoir) is βe^{V-H-K} and the steady state current $J = \beta \sum'_i P_i$ (where the sum \sum'_i runs over all configurations that contain a proton at the last site), will contain the term $\beta^{V-H-K} P_{12}$.

Monte-Carlo simulations were implemented for relatively small ($N = 10$) systems by randomly choosing a

site, and making an *allowed* transition with the probability $\xi \exp(E_i - E_f)/r_{max}$, where r_{max} is the maximum possible transition rate of the entire system. In the next time step, a particle is again chosen at random and its possible moves are evaluated. The currents were computed after the system reached steady-state by counting the net transfer of protons across all interfaces (which separate adjacent sites and the reservoirs) and dividing by $N + 1$. Physical values of J are recovered by multiplying by r_{max} . Particle occupation statistics within the chain were tracked by using the definitions of $+$, 0 and $-$ particle densities at each site i : $\rho_+(i) = \langle \sigma_i(\sigma_i + 1)/2 \rangle$, $\rho_0(i) = \langle (1 - \sigma_i^2) \rangle$, and $\rho_-(i) = \langle \sigma_i(\sigma_i - 1)/2 \rangle$, respectively. However, for our subsequent discussion, it will suffice to analyze simply the chain-averaged proton concentration $\bar{\sigma}_0 = \sum_{i=1}^N \rho_0(i)$. All MC results were checked and compared with the exact numerical results from the three-site, 27-state master equation.

RESULTS AND DISCUSSION

Here, we present MC simulation results for a lattice of size $N = 10$. The mechanisms responsible for the different qualitative behaviors are revealed and the effects of each interaction term will be systematically analyzed. We explore a range of relative kinetic rates, all nondimensionalized in units of p_0 , the intrinsic proton hopping rate from between adjacent waters. Estimates for p_0 derived from quantum MD simulations are on the order of 1ps^{-1} [Sadeghi & Cheng 1999, Mavri & Berendsen 1995, Mei *et al.* 1998, Schmitt & Voth 1999].

One of the main features we wish to explore is the effect of multiple proton occupancy on current-voltage relationships. To understand what values of transition rates would permit multiple proton occupancy, consider water at $\text{pH}=7$, which has 10^{-7}M proton and hydroxyls. This concentration corresponds to about $60 \text{H}_3\text{O}^+$ and 60OH^- species per cubic micron. Even at $\text{pH} 4$, one would only have $\sim 60,000$ hydroniums per μm^3 , corresponding to a typical distance between hydroniums of $\sim 25\text{nm}$. Since there are only $\sim 10 - 20$ waters within a single-file channel, and at $\text{pH} 4$, only about one in $500,000$ waters are protonated in bulk, multiple protons in a single channel can occur only if protonated species within the channel are highly stabilized by interactions with the chemical subgroups comprising the pore interior. This stabilizing effect is modeled by small escape rates β_0, γ_0 , and assumed to be distributed equally such that p_0 remains constant across all sites within the lattice. Although from a concentration point of view, small entrance rates α_0, δ_0 arise from infrequent protons that wander into the first site of the channel, their exit rates β_0, γ_0 can be suppressed even more by their stabilization once inside the channel. In all of our simulations, we will assume proton stabilization is moderately strong and limit ourselves rates $\beta_0, \gamma_0 < \alpha_0, \delta_0$. The values we use give steady-state proton occupancies across the whole range of values from $\lesssim 1$ to N .

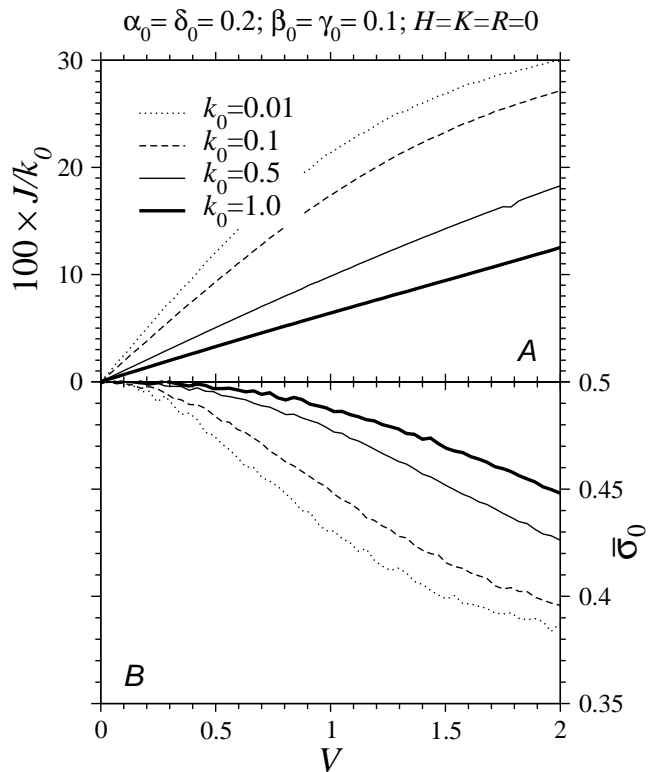


FIG. 4: Saturation due to small flip rates $k_+ = k_- = k_0$. Currents and rates in all plots are nondimensionalized by units of p_0 . (A) Small k_0 determines the rate limiting step whereupon increasing V does little to increase the current. Increasing k_0 pushes the sublinear (saturation) regime of the $J - V$ relationship to larger values of voltage V . (B) The total proton occupancy decreases with decreasing k_0 .

First consider symmetric solutions and featureless, uniform pores where $\alpha_0 = \delta_0, \beta_0 = \gamma_0$. The only possible driving force is an external voltage V . In Fig. 4, we plot the current-voltage relationship for various flipping rates k_0 . We initially ignore interaction effects and set $H = K = R = 0$. Currents for sufficiently small V are always nearly linear. However, for sufficiently large V , the rate limiting step eventually becomes the water flipping rate k_0 . Further increases in V do not increase the overall steady-state current, and the current-voltage curve becomes sublinear before saturating. The crossover to sublinear (water flipping rate limited) behavior depends on the value of k_0 , with sublinear onset occurring at higher voltages V for larger k_0 . In the noninteracting case, for most reasonable values of rate constants, any possible superlinear regime does not arise as it is washed out by the sublinear, water flip rate-limited saturation. The only instance found where noticeable superlinear behavior in the steady-state proton current arises is in the limit of large k_0 and when $\alpha_0, \delta_0, p_0 \ll \beta_0, \gamma_0$. For the parameters explored, the currents J increase with increasing k_0 (Fig. 4A); thus, the mean proton occupancies are *qualitatively* consistent with dynamics limited by internal

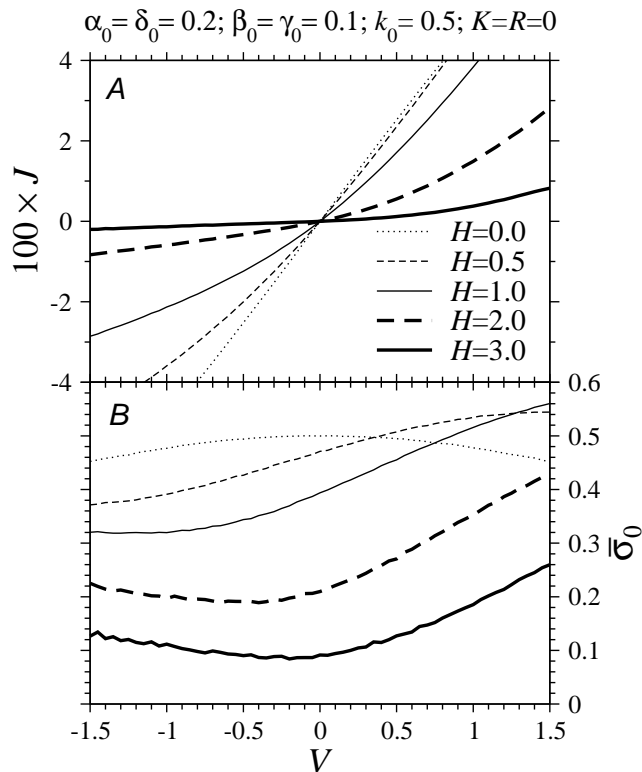


FIG. 5: Currents (A) and averaged proton occupation (B) in the presence of a constant water dipole-aligning field $H > 0$. For larger V , the V -independent H assumption used in this scenario will break down due to the orientation effects of V on the water dipoles.

proton hops. For small flipping rates, successive entry of protons is slow, while exit is not affected. As k_0 is increased, the bottlenecks near the entrance are relieved to a greater degree than those near the exit, increasing the overall proton occupancy (cf. Fig. 4B).

Figure 5 displays the effects of a fixed, external, dipole-orienting field $H \neq 0$. All other interactions and fields, except the external driving voltage V , are turned off. The convention used in the energy Eq. 1 favors a “+” state for $H > 0$. This asymmetry leads to an asymmetry in the $J - V$ relationship (Fig. 5A). After an initial proton has traversed the channel, flipping of the “-” waters left in its wake is suppressed for $H > 0$, thereby preventing further net proton movement. The persistent blockade induced by increasing H is evident in Fig. 5B where the proton density decreases for increasing H .

Although H is held fixed in Fig. 5, physically, dipole alignment fields arise from external electric fields that couple to the permanent dipoles of water. Therefore, we expect that $H = L_{HV}V$ where L_{HV} represents the orientational polarizability of the water molecule. It has been conjectured that when L_{HV} is positive (defined as preferring waters with lone pairs pointing to the left, or in the “+” state), the current should increase superlinearly with V since waters ahead of any proton will be oriented prop-

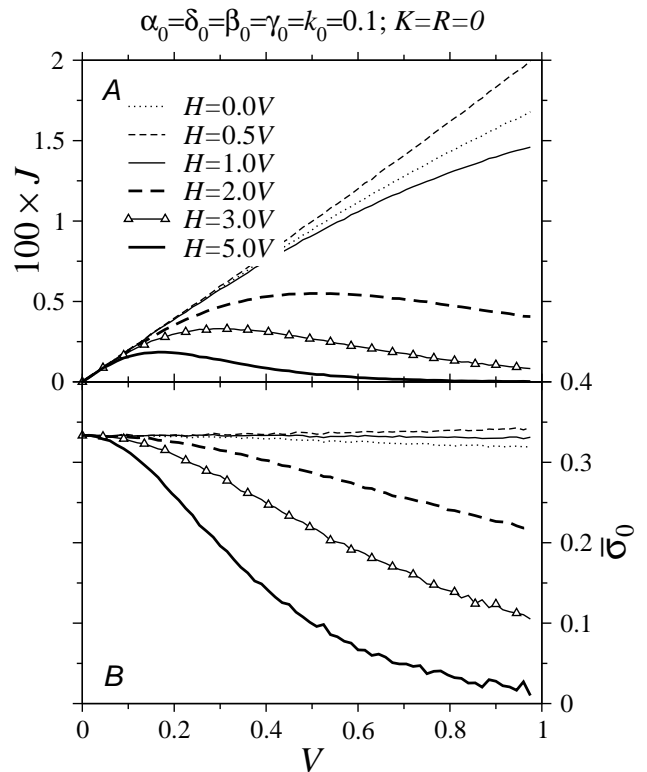


FIG. 6: (A) Negative differential resistance (NDR) for large L_{HV}, V . Although transitions such as $\dots - +0 - + \dots \rightarrow \dots - +0 + + \dots$ are accelerated, giving rise to a state where proton transport to the right is possible, NDR can arise because transitions such as $\dots - +0 + + \dots \rightarrow \dots - + - 0 + \dots$ created an additional “-” particle and is disfavored. (B) The average proton occupation *decreases* as V for large L_{HV} .

erly as to receive it. Figure 6 shows the current-voltage relationship for various L_{HV} . Although for very small L_{HV} , the current does increase very slightly, it becomes severely sublinear for larger L_{HV} and V . In fact, it can attain a negative differential resistance (NDR) similar to that found in Gunn diodes or other “negistor” devices. The physical origins of NDR in proton conduction arise from the energetic cost of producing a “-” state as a proton moves forward. Although the path ahead of the proton is biased to “+” states, the proton transfer step as defined in our model *necessarily* leaves behind a “-” particle. Thus, although the field $H = L_{HV}V$ properly aligns waters ahead of a proton, it also provides an energetic cost for the tail of “-” particles left by a forward-moving proton. This energetic penalty inhibits the proton from moving forward despite the direct driving force V acting on it.

The average density plotted in Fig. 6B decreases as V or large L_{HV} . Large L_{HV} not only hinders forward proton hops, but enhances backward hops of protons that have just hopped forward during its previous time step. Proton dynamics are slowed dramatically, and only at the last site can they exit the pore. Proton entry from

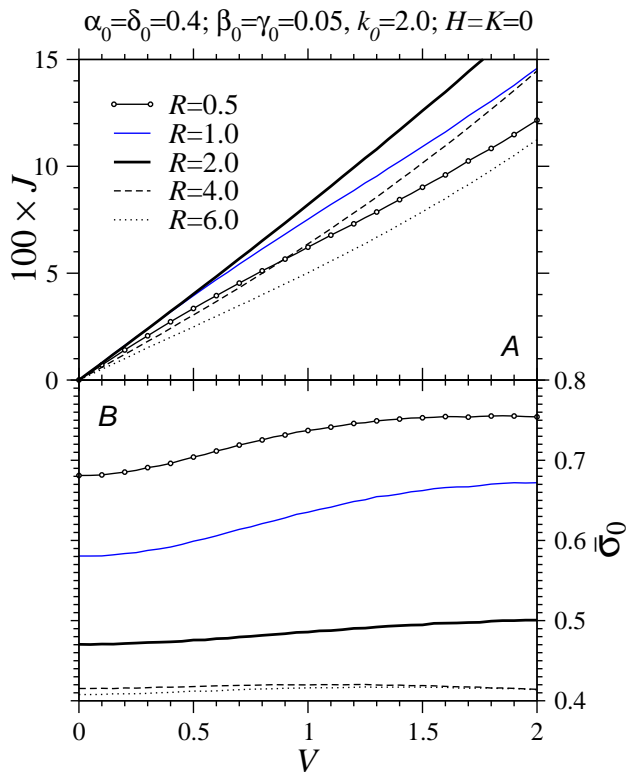


FIG. 7: The effects of increasing nearest-neighbor proton-proton repulsion within the chain. Fixed parameters are $\alpha_0 = \delta_0 = 0.4$, $\beta_0 = \gamma_0 = 0.05$, $k_0 = 2.0$, and $H = K = 0$. (A) The onset of sublinear behavior in the $J - V$ relationship is delayed for larger repulsions R , making the curves appear locally more superlinear. (B) The average proton densities per site. For small R , although densities are high, increasing V increases the clearance rate near the entrance such that the effectively increased injection increases overall proton density. At higher repulsions R , the clearance effects is not as strong and the simultaneously increased extraction rate prevents a large increase in the overall proton density.

the left reservoir on the other hand, is often quickly followed by exit back into the left reservoir. The protons are *effectively* entry-limited, and the density is rather low. As V increases, the dynamics become even more “entry-limited,” and the overall proton occupancy decreases.

The effects of proton-proton repulsion ($R > 0$) are considered in Figs 7 and 8. These simulations are consistent with the hypothesis that proton-proton repulsions can give rise to superlinear current [Hille & Schwarz 1978]. Figure 7A shows a slight preference for superlinear behavior as repulsion R is increased. Not surprisingly, Fig. 7B shows that the overall density of protons within the pore decreases with increasing repulsion.

The sublinear-to-superlinear behavior as the proton concentration in the identical reservoirs is increased is shown in Fig. 8A. Although for these parameters, the effect is not striking, there is indeed a trend away from sublinear behavior as pH is decreased, or, as $\alpha_0 = \delta_0$ is increased. Mea-

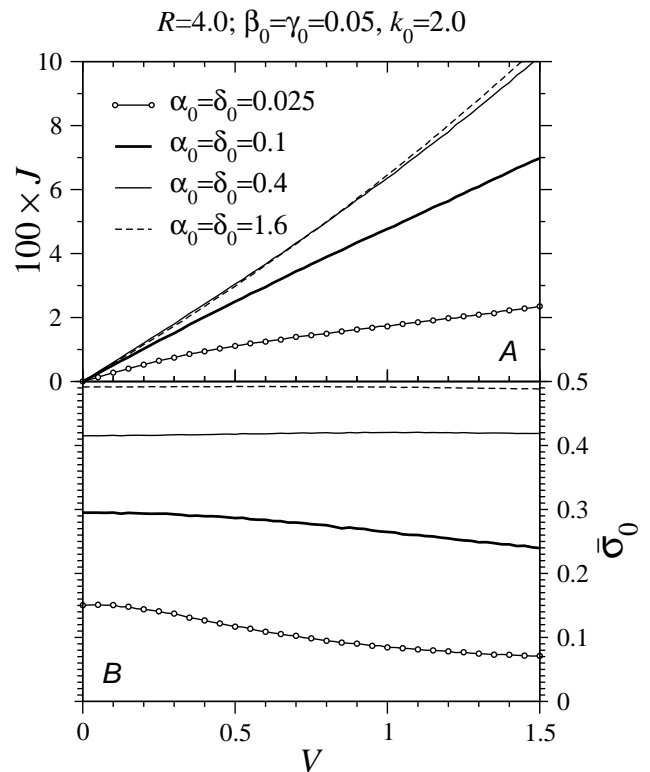


FIG. 8: Transition from sublinear to superlinear current behavior as proton concentration in the symmetric reservoirs is increased. (A) $J - V$ relationship for various concentrations $\alpha_0 = \delta_0$ for fixed $H = K = 0$, $R = 4.0$, $\beta_0 = \gamma_0 = 0.05$, and $k_0 = 2.0$. (B) The averaged proton concentration σ_0 at each lattice site as a function of driving voltage. The concentrations increase for all ranges of V as $\alpha = \delta$ is increased.

surements, though, also show rather modest superlinear behavior [Eisenman *et al.* 1980, Phillips *et al.* 1999, Rokitskaya *et al.* 2002]. The occupancy also increases with decreasing pH, enhancing the effect of proton-proton repulsion. These behaviors are consistent with experimental findings [Eisenman *et al.* 1980] and those in the simulations depicted in Fig. 7 where increased repulsion exhibited superlinear $J - V$ curves.

Finally, we consider the effects of dipole coupling $K \neq 0$ between adjacent water molecules. This interaction is analogous to a nearest neighbor ferromagnetic coupling in *e.g.*, Ising models. Fig. 9A shows that for sufficiently large $\alpha_0 = \delta_0$, a superlinear behavior arises (for small enough V and large enough k_0 such that saturation has not yet occurred). Notice that as $\alpha_0 = \delta_0$ is increased, the $J - V$ relationship can become more sublinear before turning superlinear. Here, we have used a higher value of k_0 to suppress sublinear behavior to larger V , but the qualitative shift from sublinear to slightly superlinear behavior exists for small k_0 . Moreover, recent comparisons between gramicidin A and gramicidin M channels suggest that water reorientation is not rate-limiting [Gowen *et al.* 2002]. The nature of the superlinear be-

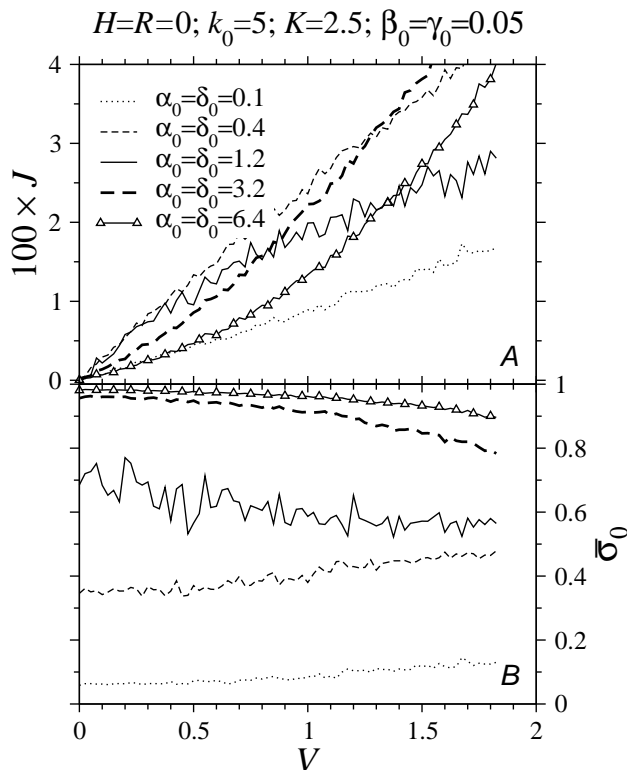


FIG. 9: (A) The current-voltage relationship for various proton injection rates in the presence of ferromagnetic water dipole coupling. (B) Mean proton occupations increase with increasing injection rates.

havior can be deduced from Fig. 9B, where the mean proton density is shown to increase with $\alpha_0 = \delta_0$. Waters that neighbor a proton are relieved of their dipolar coupling and can more readily flip to a configuration that would allow acceptance of another proton. For example, the transition $\dots 0 - 0 \dots \rightarrow \dots 0 + 0 \dots$ will occur faster than $\dots - 0 \dots \rightarrow \dots - + 0 \dots$. This lubrication effect arises only when the proton density is high and $K \neq 0$.

SUMMARY AND CONCLUSIONS

We have developed a lattice model for proton conduction that quantifies the kinetics among three approximate states of the individual water molecules inside a simple, single-file channel such as gramicidin A. The three states represent water molecules with left and right-pointing water dipoles, and protonated ions. Our approach allows us to explore the *steady-state* behavior of proton currents, occurring over timescales inaccessible by MD simulations. The model, along with analyses of Monte-Carlo simulations, also extends analytic models [Schumaker *et al.* 2000, Schumaker *et al.* 2001] to include multiple proton occupancy and the memory effects of protons that have recently traversed the water-wire. Monte-Carlo simulations of the lattice model was performed to test conjectures on a number of observed qualitative features in proton transport across water wires.

Four interaction energies that modify the kinetic rates are considered: A dipole-orienting field which tends to align the water molecules, a ferromagnetic dipole-dipole interaction terms between neighboring water molecules, a penalty from the repulsion between neighboring protons, and an external electric field (transmembrane potential) that biases the hops of the charged protons.

We find current-voltage relationships that can be both superlinear and sublinear depending on the voltage V . For large enough voltages, the proton hopping step is no longer rate limiting. Water flipping rates limit proton transfer and further increases in V do little to increase the steady-state proton current J . This observation suggests that the observed transition from sublinear to superlinear behavior can be effected by varying an *effective* water flipping rate. Although we find that indeed proton-proton repulsion can lead to slightly superlinear $J - V$ characteristics, particularly for large repulsions and proton injection rates (low pH).

Dipole-dipole interactions between neighboring waters are also incorporated. Previous single-proton theories [Schumaker *et al.* 2000, Schumaker *et al.* 2001] have considered the propagation of a single defect back and forth in the pore. In our model, the number of protons and defects are dynamical variables that depend on the injection rates and the dipole-dipole coupling, respectively. For large coupling K , we expect very few defects, and effective water flipping rates will be low. However, when injection rates and proton occupancy in the pore is high, some dipole-dipole couplings are broken up by the intervening protons. Thus, protons can “lubricate” their neighboring dipoles, allowing them to flip faster than if they were neighboring a dipole pointed in the same direction. Using simulations, we showed that this lubrication effect can give rise to a superlinear $J - V$ relationship

Although the parameters used in our analyses can be further refined by estimating them from shorter time MD simulations, or other continuum approaches [Edwards *et al.* 2002, Partenskii & Jordan 1992]. More complicated local interactions with membrane lipid dipoles [Rokitskaya *et al.* 2002] and internal pore constituents (such as Trp side groups [Dorigo *et al.* 1999, Gowen *et al.* 2002]) can be incorporated by allowing H, K, p_0 and/or k_0 to reflect the local molecular environment by varying along the lattice site (position) within the channel [Kolomeisky 1998].

The author thanks Mark Schumaker for vital discussions and comments on the manuscript. This work was performed with the support of the National Science Foundation through grant DMS-0206733, and the National Institutes of Health through grant R01 AI41935.

APPENDIX A: NOINTERACTING MEAN-FIELD RESULTS

For the sake of completeness, and as a guide to aid qualitative understanding, we review analytic results in the case $R = K = H = 0$, where only exclusions are included. Some of these results have been derived previously using mean-field approximations [Chou 2002].

If $V = 0$ ($\xi = \xi_0$), only pH differences between the two reservoirs can affect a nonzero steady-state proton current. The proton concentration difference is reflected by a difference between the entry rates from the two reservoirs $\alpha_0 \neq \delta_0$, and the steady-state current can be expanded in powers of $1/N$: $J = a_1/N + a_2/N^2 + \mathcal{O}(N^{-3})$. In the long chain limit, we found [Chou 2002]

$$J \sim \frac{k_+ k_-}{N(k_+ + k_-)} \times \ln \left[\frac{\beta(k_+ + k_-) + k_+ \delta}{\gamma(k_- + k_+) + k_- \alpha} \frac{\gamma(k_+ + k_-) + \alpha(p_- + k_-)}{\beta(k_+ + k_-) + k_+ \delta(p_- / k_- + 1)} \right] + \mathcal{O}(N^{-2}). \quad (\text{A1})$$

For channels with reflection-symmetric molecular structures, $\beta_0 = \gamma_0$, and Eq. A1 can be further simplified by expanding in powers of $k_- \alpha - k_+ \delta$,

$$J \sim \frac{\beta p_+ k_- (k_- \alpha - k_+ \delta)}{N [\beta(k_- + k_+) + k_+ \delta] (\beta + \delta)(k_+ + k_-)} + \mathcal{O}((k_- \alpha - k_+ \delta)^2) + \mathcal{O}(1/N^2), \quad (\text{A2})$$

Finally, in the *large* α and $\delta = 0$ limit,

$$J \sim \frac{k_+ k_-}{(k_+ + k_-) N} \log \left(1 + \frac{p_-}{k_+} \right) - \frac{\gamma k_+ k_- p_-}{\alpha N (k_+ + k_-)(k_+ + p_-)} + \mathcal{O}(\alpha^{-2} N^{-1}). \quad (\text{A3})$$

For driven systems, where, say, $\alpha > \delta, \beta > \gamma$, and $p_+ > p_-$, a finite current persists in the $N \rightarrow \infty$ limit. We can use mean-field approximations familiar in the totally asymmetric simple exclusion process (TASEP) [Derrida 1998, Schutz & Domany 1993] to conjecture that three current regimes exist. If the both proton entry and exit is fast, and the rate-limiting steps involve water flipping, or interior protons hops with rate p_+ , we expect that a maximal current regime exists and that the densities of the three states along the interior of a long chain are spatially uniform. Mean-field analysis from previous work [Chou 2002] yields

$$J = \frac{2(p_+ k_- - p_- k_+)}{(p_+ + p_-)^2} \left[\frac{(p_- + p_+)}{2} + k_- + k_+ - \sqrt{k_+ + k_-} \sqrt{k_- + k_+ + p_+ + p_-} \right]. \quad (\text{A4})$$

For a purely asymmetric process, $p_- = 0$, and the current approaches the analogous maximal-current expression of the single species TASEP,

$$J(p_- = 0) \sim \frac{p_+ k_-}{4(k_- + k_+)} + \mathcal{O}\left(\frac{p_+}{k_-}\right), \quad (\text{A5})$$

except for the additional factor of $k_-/(k_- + k_+)$ representing the approximate fraction of time sites ahead of a proton are in the $+$ configuration. These approximations neglect the influence of protons that have recently passed, temporarily biasing the water to be in a “ $-$ ” configuration. Therefore, it is not surprising that these results are accurate only in the $k_+, k_- \gg p$ limit.

A similar approach is taken when the currents are entry or exit limited. From the mean-field approximation of the steady-state equation for ρ_{\pm} near the channel entry,

$$\begin{aligned} \frac{\partial \rho_-}{\partial t} &= p_+ \rho_0 \rho_+ + k_+ \rho_+ - k_- \rho_- = 0 \\ \frac{\partial \rho_+}{\partial t} &= -\alpha \rho_+ - k_+ \rho_+ + k_- \rho_- = 0, \end{aligned} \quad (\text{A6})$$

where we have for simplicity set $p_- = \gamma = 0$. Upon using normalization $\rho_- + \rho_0 + \rho_+ = 1$, and Eqs. A6, we find the mean densities near the left boundary

$$\begin{aligned} \rho_- &= \frac{(\alpha + k_-)(p_+ - \alpha)}{p_+(\alpha + k_- + k_+)}, \\ \rho_+ &= \frac{k_-(p_+ - \alpha)}{p_+(\alpha + k_- + k_+)}, \end{aligned} \quad (\text{A7})$$

and the approximate entry rate-limited steady-state current

$$J \approx p_+ \rho_0 \rho_+ = \alpha \rho_+ = \frac{\alpha k_- (1 - \alpha/p)}{(\alpha + k_- + k_+)}. \quad (\text{A8})$$

This result resembles the steady-state current of the low density phase in the simple exclusion process [Derrida 1998, Chou 2003], except for the factor $k_-/(\alpha + k_- + k_+)$ representing the fraction of time the first site is in the $+$ state, and able to accept a proton from the left reservoir.

When the rate β is rate-limiting, we consider the mean-field equations near the exit of the channel

$$\begin{aligned} \frac{\partial \rho_-}{\partial t} &= \beta \rho_0 + k_+ \rho_+ - k_- \rho_- = 0 \\ \frac{\partial \rho_+}{\partial t} &= -p_+ \rho_0 \rho_+ + k_- \rho_- - k_+ \rho_+ = 0, \end{aligned} \quad (\text{A9})$$

and their solutions

$$\rho_- = \frac{\beta(k_+ + p_+ - \beta)}{p_+(k_- + \beta)}, \quad \rho_+ = \frac{\beta}{p_+}. \quad (\text{A10})$$

The exit-limited steady-state current is thus

$$J \approx \beta\rho_0 = \frac{\beta}{k_- + \beta} \left(k_- - \frac{\beta(k_- + k_+)}{p_+} \right). \quad (\text{A11})$$

The results above are derived from mean-field assumptions which neglect correlations in particle occupancy between neighboring sites. Although mean-field theory

happens to give exact results for the simple exclusion process, the results above are only exact in the large k_{\pm}/p_{\pm} limit, as has been shown by Monte-Carlo simulations [Chou 2002]. Only in this limit, where the memory of a previously passing proton is quickly erased, are the mean-field results quantitatively accurate [Chou 2002]. Nonetheless, the mean-field calculations of the simplified system ($H = K = R = 0$) yields qualitatively correct results for the steady-state current, provides a connection with well-known results of the TASEP, and gives an explicit qualitative description of the mechanisms at play.

-
- [Agmon 1995] Agmon, N. 1995. The Grotthuss mechanism. *Chem. Phys. Lett.* 244:456-462.
- [Alberts *et al.* 1994] B. Alberts, D. Bray, J. Lewis, M. Raff, K. Roberts and J. D. Watson, *Molecular biology of the cell*, (Garland Publishing, New York, 1994).
- [Akeson & Deamer 1991] Akeson, M., and D. W. Deamer. 1991. Proton conductance by the gramicidin water wire: Model for proton conductance in the F1F0 ATPases? *Biophys. J.*, 60:101-109.
- [Anderson 1983] Andersen, O. S. 1983. Ion movement through gramicidin A channels. Single-channel measurements at very high potentials. *Biophys. J.*, 41:119-133.
- [Bala *et al.* 1994] Bala, P., B. Lesyng, and J. A. McCammon. 1994. Applications of quantum-classical and quantum-stochastic molecular dynamics for proton transfer processes. *Chem. Phys.* 180:271-285.
- [Boyer 1997] Boyer, P. 1997. The ATP synthase - a splendid molecular machine. *Annu. Rev. Biochem.* 66:717-749.
- [Busath *et al.* 1998] Busath, D. D., C. D. Thulin, R. W. Hendershot, L. R. Phillips, P. Maughn, C. D. Cole, N. C. Bingham, S. Morrison, L. C. Baird, R. J. Hendershot, M. Cotten, and T. A. Cross. 1998. Non-contact dipole effects on channel permeation. I. Experiments with (5F-indole)Trp-13 gramicidin A channels. *Biophys. J.* 75:2830-2844.
- [Chernyshev & Cukierman 2002] Chernyshev, A. and S. Cukierman. 2002. Thermodynamic View of Activation Energies of Proton Transfer in Various Gramicidin A Channels. *Biophys. J.* 82:182-192.
- [Chou 1998] Chou, T. 1998. How Fast do Fluids Squeeze Through Microscopic Single-File Channels? *Phys. Rev. Lett.* 80:85-89.
- [Chou 1999] Chou, T. 1999. Kinetics and thermodynamics across single-file pores: solute permeability and rectified osmosis. *J. Chem. Phys.* 110:606-615.
- [Chou & Lohse 1999] Chou, T. and D. Lohse. 1999. Entropy-driven pumping in zeolites and ion channels. *Phys. Rev. Lett.* 82:3552-3555.
- [Chou 2002] Chou, T. 2002. A spin flip model for one-dimensional water wire proton transport. *J. Phys. A.* 35:4515-4526.
- [Chou 2003] Chou, T. 2003. Ribosome recycling, diffusion, and mRNA loop formation in translational regulation. *Biophys. J.* 85:755-773.
- [Cotten *et al.* 1999] Cotten, M., C. Tian, D. D. Busath, R. B. Shirts, and T. A. Cross. 1999. Modulating dipoles for structure-function correlations in the gramicidin A channel. *Biochemistry.* 38:9185-9197.
- [Cukierman 1997] Cukierman, S., E. P. Quigley, and D. S. Crumrine. 1997. Proton conductance in gramicidin A and its dioxolane-linked dimer in different bilayers. *Biophys. J.* 73:2489-2502.
- [Deamer 1987] Deamer, D. W. 1987. Proton permeation of lipid bilayers. *J. Bioenerg. Biomembr.* 19:457-479.
- [Decornez 1999] Dcornez, H., K. Drukker, and S. Hammes-Schiffer. 1999. Solvation and hydrogen-bonding effects on proton wires. *J. Phys. Chem. A.* 103:2891-2898.
- [Derrida 1998] Derrida, B. 1998. An exactly soluble non-equilibrium system: The asymmetric simple exclusion process. *Physics Reports* 301:65-83.
- [DeCoursey & Cherny 1994] DeCoursey, T. E., and V. V. Cherny. 1994. Voltage-activated hydrogen ion currents. *J. Membr. Biol.* 141:203-223.
- [Dorigo *et al.* 1999] Dorigo, A. E., D. G. Anderson, and D. D. Busath. 1999. Noncontact dipole effects on channel permeation. II. Trp conformations and dipole potentials in gramicidin A. *Biophys. J.* 76:1897-1908.
- [Edwards *et al.* 2002] Edwards, S., B. Corry, S. Kuyucak, and S.-H. Chung. 2002. Continuum Electrostatics Fails to Describe Ion Permeation in the Gramicidin Channel. *Biophys. J.* 83: 1348 - 1360.
- [Eisenman *et al.* 1980] Eisenman, G., B. Enos, J. Hägglund, and J. Sandblom. 1980. Gramicidin as an example of a single-filing ionic channel. *Ann. N.Y. Acad. Sci.* 339:8-20.
- [Fisher & Kolomeisky 1999] Fisher, M. E., and A. B. Kolomeisky. 1999. The force exerted by a molecular motor. *Proc. Natl Acad. Sci. USA.* 96:6597-6602.
- [Grabe & Oster 2001] Grabe, M. and G. Oster. 2001. Regulation of Organelle Acidity. *J. Gen. Physiol.* 117:329-343.
- [Gowen *et al.* 2002] Gowen, J. A., J. C. Markham, S. E. Morrison, T. A. Cross, D. A. Busath, E. J. Mapes, and M. F. Schumaker. 2002. The Role of Trp Side Chains in Tuning Single Proton Conduction through Gramicidin Channels. *Biophys. J.* 83:880-898.
- [Grotthuss 1806] Grotthuss, C. J. T. 1806. Sur la décomposition de l'eau et des corps qu'elle tient en dissolution à l'aide de l'électricité galvanique, *Ann. Chim.* 58:54-74.
- [Hille & Schwarz 1978] Hille, B., and W. Schwarz. 1978. Potassium channels as multi-ion single-file pores. *J. Gen. Physiol.* 72:409-442.

- [Hladky & Haydon 1972] Hladky, S. B., and D. A. Haydon. 1972. Ion transfer across lipid membranes in the presence of gramicidin A. I. Studies of the unit conductance channel. *Biochim. Biophys. Acta.* 274:294-312.
- [Hu & Cross 1995] Hu, W., and T. A. Cross. 1995. Tryptophan hydrogen bonding and electrical dipole moments: functional roles in the gramicidin channel and implications for membrane proteins. *Biochemistry.* 34:14147-14155.
- [Hummer *et al.* 2001] Hummer, G., J. C. Rasaiah, and J. P. Noworyta. 2001. Water conduction through the hydrophobic channel of a carbon nanotube. *Nature* 414:188-190.
- [Jordan 1984] Jordan, P. C. 1984. The total electrostatic potential in a gramicidin channel. *J. Membr. Biol.* 78:91-102.
- [Kalra *et al.* 2003] Kalra, A., S. Garde, and G. Hummer. 2003. Osmotic water transport through carbon nanotube membranes. *Proc. Natl. Acad. Sci. USA* 100:10175-10180.
- [Karimipour 1999] Karimipour, V. 1999. Multispecies asymmetric simple exclusion process and its relation to traffic flow *Phys. Rev. E* 59:205-212.
- [Kolomeisky 1998] Kolomeisky, A.B. 1998. Asymmetric simple exclusion model with local inhomogeneity. *J. Phys. A: Math. Gen.* 31:1153-1164.
- [Lanyi 1995] Lanyi, J. K. 1995. Bacteriorhodopsin as a model for proton pumps. *Nature.* 375:461-463.
- [Levitt *et al.* 1978] Levitt, D. G., S. R. Elias, and J. M. Hautman. 1978. Number of water molecules coupled to the transport of sodium, potassium and hydrogen ions via gramicidin, nonactin or valinomycin. *Biochim. Biophys. Acta.* 512:436-451.
- [Lynden-Bell & Rasaiah 1996] Lynden-Bell, R. M., and J. C. Rasaiah. 1996. Mobility and solvation of ions in channels. *J. Chem. Phys.* 105:9266-9280.
- [MacDonald & Gibbs 1969] MacDonald, C. T. and J. H. Gibbs. 1969. Concerning the Kinetics of Polypeptide Synthesis on Polyribosomes. *Biopolymers*, 7:707-725.
- [Marx *et al.* 1999] Marx, D., M. E. Tuckerman, J. Hutter, and M. Parrinello. 1999. The nature of the hydrated excess proton in water. *Nature.* 397:601-604.
- [Mavri & Berendsen 1995] Mavri, J., and H. J. C. Berendsen. 1995. Calculation of the proton transfer rate using density matrix evolution and molecular dynamics simulations: inclusion of the proton excited states. *J. Phys. Chem.* 99:12711-12717.
- [Mei *et al.* 1998] Mei, H. S., M. E. Tuckerman, D. E. Sagnell, and M. L. Klein. 1998. Quantum nuclear ab initio molecular dynamics study of water wires. *J. Phys. Chem. B.* 102:10446-10458.
- [Nagle 1987] Nagle, J. F. 1987. Theory of passive proton conductance in lipid bilayers. *J. Bioenerg. Biomembr.* 19:413-426.
- [Nagle & Horowitz 1978] Nagle, J. F., and H. J. Morowitz. 1978. Molecular mechanisms for proton transport in membranes. *Proc. Natl. Acad. Sci. USA.* 75:298-302.
- [Nagle & Tristan-Nagle 1983] Nagle, J. F., and S. Tristram-Nagle. 1983. Hydrogen bonded chain mechanisms for proton conduction and proton pumping. *J. Membr. Biol.* 74:1-14.
- [Partenskii & Jordan 1992] Partenskii, M. B., and P. C. Jordan. 1992. Nonlinear dielectric behavior of water in transmembrane ion channels: ion energy barriers and the channel dielectric constant. *J. Chem. Phys.* 96:3906-3910.
- [Phillips *et al.* 1999] Phillips, L. R., C. D. Cole, R. J. Henderson, M. Cotten, T. A. Cross, and D. D. Busath. 1999. Noncontact Dipole Effects on Channel Permeation. III. Anomalous Proton Conductance Effects in Gramicidin. *Biophys. J.* 77:2492-2501.
- [Pomès & Roux 1996] Pomès, R., and B. Roux. 1996. Structure and dynamics of a proton wire: A theoretical study of H⁺ translocation along the single-file water chain in the gramicidin A channel. *Biophys. J.* 71:19-39
- [Pomès & Roux 1998] Pomès, R., and B. Roux. 1998. Free energy profiles for H⁺ conduction along hydrogen-bonded chains of water molecules. *Biophys. J.* 75:33-40.
- [Prokop & Skala 1994] Prokop, P., and L. Skála. 1994. Theory of proton transport along a hydrogen bond chain in an external field. *Chem. Phys. Lett.* 223:279-282.
- [Rokitskaya *et al.* 2002] Rokitskaya, T. I., E. A. Kotova, and Y. N. Antonenko. 2002. Membrane Dipole Potential Modulates Proton Conductance through Gramicidin Channel: Movement of Negative Ionic Defects inside the Channel. *Biophys. J.* 82:865-873.
- [Sadeghi & Cheng 1999] R. R. Sadeghi and H.-P. Cheng. 1999. The dynamics of proton transfer in a water chain. *J. Chem. Phys.* 111:2086-2094.
- [Sagnella *et al.* 1996] Sagnella, D. E., K. Laasonen, and M. L. Klein. 1996. Ab initio molecular dynamics study of proton transfer in a polyglycine analog of the ion channel gramicidin A. *Biophys. J.* 71:1172-1178.
- [Sagnella & Voth 1996] Sagnella, D. E., and G. A. Voth. 1996. Structure and dynamics of hydronium in the ion channel gramicidin A. *Biophys. J.* 70:2043-2051
- [Scheiner 1985] Scheiner, S. 1985. Theoretical studies of proton transfers. *Acc. Chem. Res.* 18:174-180.
- [Schmitt & Voth 1999] Schmitt, U. W., and G. A. Voth. 1999. The computer simulation of proton transport in water. *J. Chem. Phys.* 111:9361-9381.
- [Schreckenber *et al.* 1995] Schreckenber, M., A. Schadschneider, K. Nagel, and N. Ito. 1995. *Phys. Rev. E* 51:2939-2949.
- [Schumaker *et al.* 2000] Schumaker, M. F., R. Pomès, and B. Roux. 2000. A Combined Molecular Dynamics and Diffusion Model of Single-Proton Conduction through Gramicidin. *Biophys. J.* 78:2840-2857.
- [Schumaker *et al.* 2001] Schumaker, M. F. and R. Pomès, and B. Roux. 2001. Framework Model For Single Proton Conduction through Gramicidin, *Biophys. J.* 80:12-30.
- [Schütz & Domany 1993] Schütz, G. and E. Domany. 1993. Phase Transitions in an Exactly Soluble One-Dimensional Exclusion Process. *J. Stat. Phys.* 72:277-296.
- [Syganow & von Kitzing 1999] A. Syganow and E. von Kitzing. 1999. (In)validity of the Constant Field and Constant Currents Assumptions in Theories of Ion Transport. *Biophys. J.* 76:768-781.
- [Wu & Voth 2003] Wu, Y., and G. A. Voth. 2003. A Computer Simulation Study of the Hydrated Proton in a Synthetic Proton Channel. *Biophys. J.* 85:864-875.

Water alignment, dipolar interactions, and multiple proton occupancy during water-wire proton transport

Tom Chou

Dept. of Biomathematics and IPAM, Los Angeles, CA 90095-1766

(Dated: September 22, 2003)

A discrete multistate kinetic model for water-wire proton transport is constructed and analyzed using Monte-Carlo simulations. The model allows for each water molecule to be in one of three states: oxygen lone pairs pointing leftward, pointing rightward, or protonated (H_3O^+). Specific rules for transitions among these states are defined as protons hop across successive water oxygens. We then extend the model to include water-channel interactions that preferentially align the water dipoles, nearest-neighbor dipolar coupling interactions, and coulombic repulsion. Extensive Monte-Carlo simulations were performed and the observed qualitative physical behaviors discussed. We find the parameters that allow the model to exhibit superlinear and sublinear current-voltage relationships and show why alignment fields, whether generated by interactions with the pore interior or by membrane potentials *always* decrease the proton current. The simulations also reveal a “lubrication” mechanism that suppresses water dipole interactions when the channel is multiply occupied by protons. This effect can account for an observed sublinear-to-superlinear transition in the current-voltage relationship.

Keywords: proton transport, asymmetric exclusion process, water wire

INTRODUCTION

The transport of protons in aqueous media and across membranes is a fundamental process in chemical reactions, solvation, and pH regulation in cellular environments [Alberts *et al.* 1994, Grabe & Oster 2001]. Proton transport in confined geometries is also relevant for ATP synthesis [Boyer 1997] and light transduction by bacteriorhodopsin [Lanyi 1995]. In this paper, we develop a lattice model for describing proton transport in *one-dimensional* environments. This study is motivated by numerous measurements of proton conduction across channels embedded in lipid membranes [Akeson & Deamer 1991, Busath *et al.* 1998, Cotten *et al.* 1999, Cukierman 1997, Deamer 1987, Eisenman *et al.* 1980]. Experiments are typically performed using membrane-spanning gramicidin channels that are only a few Angstroms in diameter. This geometric constraint imposes a single-file structure on the configurations of the interior water molecules [Hille & Schwarz 1978, Hladky & Haydon 1972].

Under the same electrochemical potential gradients, conduction of protons across ion channels occurs at a rate typically an order of magnitude higher than that of other small ions. This supports a “water-wire” mechanism [Akeson & Deamer 1991, Nagle & Horowitz 1978, Nagle & Tristan-Nagle 1983, Nagle 1987], first proposed by Grotthuss [Agmon 1995, Grotthuss 1806]. Across a water-wire, protons are shuttled across lone pairs of water oxygens as they successively protonate the waters along the single-file chain. However, since the hydrogens are indistinguishable, any one of the hydrogens in a water cluster (*e.g.*, any of the three hydrogens on a hydronium) can hop forward along the chain to protonate the next water molecule or cluster of water molecules (cf. Fig. 1). This mechanism naturally allows much faster overall con-

duction of protons compared to other small ions which have to wait for the entire chain of water molecules ahead of it to fluctuate across the pore in order to traverse the channel.

A peculiar feature of measured current-voltage relationships is a crossover from sublinear to superlinear behavior as the pH of the reservoirs is lowered. Measurements by Eisenman [Eisenman *et al.* 1980] were carried out in symmetric solutions in the 1-3 pH range, and the results were recently reproduced by Busath *et al.* [Busath *et al.* 1998] and Rokitskaya *et al.* [Rokitskaya *et al.* 2002]. These experiments were performed using simple, relatively featureless gramicidin A (gA) channels. One leading hypothesis is that the nonlinear proton current-voltage relationships arise from the intrinsic proton dynamics within such simple channels. Specifically, multiple proton occupancy and repulsion among protons within the channel may give rise to the observed nonlinearity [Hille & Schwarz 1978, Phillips *et al.* 1999, Schumaker *et al.* 2001].

There have been a number of recent theoretical studies of water-wire proton conduction. Extensive simulations on the quantum dynamics of proton exchange in essentially small, representative water clusters in vacuum have been used to predict microscopic hopping rates between water clusters [Bala *et al.* 1994, Sadeghi & Cheng 1999, Marx *et al.* 1999, Mavri & Berendsen 1995, Mei *et al.* 1998, Sagnella *et al.* 1996, Schmitt & Voth 1999]. Pomès and Roux [Pomès & Roux 1996] have performed classical molecular dynamics (MD) simulations on water-channel interactions, proton hopping, and water reorientation. They derive effective potentials of mean force describing the energy barriers encountered by a single proton within the pore. Since MD simulations are presently limited to only processes that occur over a few nanoseconds, none of these computational methods are efficient at probing very long time, steady-state transport behavior. On

In addition to proton exclusion, the transition rules are constrained by the orientation of the waters at each site and are defined in Fig. 1B. A proton can enter the first site ($i = 1$) from the left reservoir and protonate the first water molecule with rate α only if the hydrogens of the first water are pointing to the right (such that its lone-pair electrons are left-pointing, ready to accept a proton). Conversely, if a proton exits from the first site back into the left reservoir (with rate γ), it leaves the remaining hydrogens right-pointing. In the pore interiors, a proton at site i can hop to the right(left) with rate p_+ (p_-) only if the adjacent particle is a right(left)-pointing, unprotonated water molecule. If such a transition is made, the water molecule left at site i will be left(right) pointing. Physically, as a proton moves to the right, it leaves a wake of $-$ particles to its left. A left moving proton leaves a trail of $+$ particles to its right. These trails of $-$ or $+$ particles are unable to accept another proton from the same direction. Protons can follow each other successively only if water molecules can reorient such that these trails of $+$'s or $-$'s are thermally washed out. Water reorientation rates are denoted k_{\pm} (cf. Figs. 1B and 2). Protons at the rightmost end of the water wire (at site $i = N$), exit with rate β , which is different from p_+ since the local microenvironment (*e.g.*, typical distance to acceptor electrons) of the bulk waters that accept this last proton is different from that in the pore interior. From the right reservoir, protons can hop back into the water wire with rate δ if a water in the “ $-$ ” configuration is at site $i = N$. The entrance rates α and δ are functions of at least the proton concentration in the respective reservoirs. Figure 2 shows a representative time series of the evolution of a specific configuration. The rate-limiting steps in steady-state proton transfer across biological water channels are thought to be associated with water flipping [Pomès & Roux 1998].

The lattice discretization for individual H_3O^+ ions need not be interpreted literally. Larger complexes can be effectively modeled by reinterpreting p_{\pm} , k_{\pm} , and the basic unit of hopping for the proton. For example, if certain conditions obtain, where ions are predominantly two-oxygen clusters (H_5O_2^+), we defined each pair of waters as occupying a single lattice site, k_{\pm} as an effective reorientation time for the following pair of waters, and p_{\pm} as the hopping rate to an adjacent oxygen lone-pair. The Grotthuss water-wire mechanism is qualitatively preserved as long as the proper identification with the microphysics is made.

All eight “parameters” used in our model (the rates p_{\pm} , k_{\pm} , α , β , γ , δ), can be related to measured bulk quantities or derived from short-time MD simulations. They are a minimal set and are equivalent to the numerous bulk parameters used in other models [Schumaker *et al.* 2001], such as the bulk proton diffusion constant, water orientational diffusion constants, etc. Using similar MD approaches then, one should be able to approximately fix the parameters used in our model. For example, variations in the potential of mean

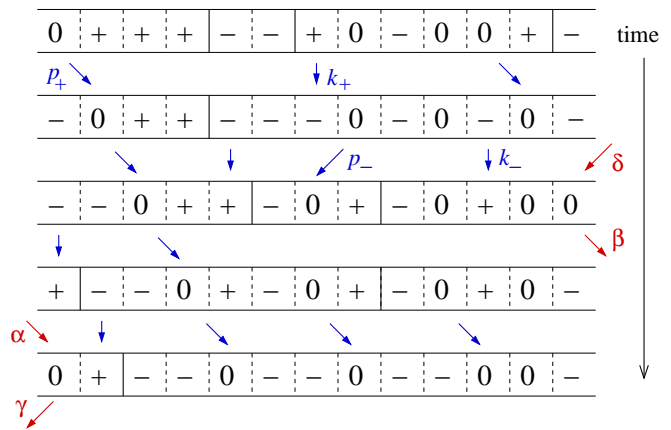


FIG. 2: A time series depicting a number of representative transitions obeying the dynamical constraints of our model. A proton (0) at site i can move to the right with rate p_+ only if site $i + 1$ is occupied by a properly aligned (lone-pair electrons pointing to the left) water molecule (+). When a proton leaves site i to the right, it leaves behind a water in state “ $-$ ”, with lone pair electrons pointing to the right. Protons at site i can also move to the left with rate p_- if site $i - 1$ is a water in the “ $-$ ” state. In this case, a water is left behind at behind site i in the “ $+$ ” state. The neutral water molecules must flip ($+$ \leftrightarrow $-$) in order for a nonzero steady-state current to exist.

- (A) ...00+0... \rightarrow ...0-00... $\Delta E = H - V$
- (B) ...00+-... \rightarrow ...0-0-... $\Delta E = H - K - R - V$
- (C) ...+++... \rightarrow ...+-+... $\Delta E = H + 2K$
- (D) ...00++... \rightarrow ...0-0+... $\Delta E = H + K - R - V$

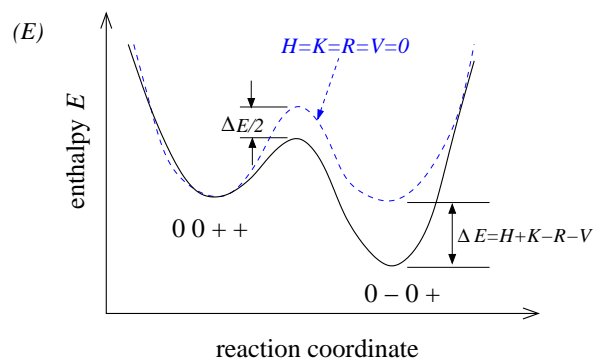


FIG. 3: (A – D) Energy differences between final and initial states which involve a change in ferroelectric coupling, net dipole moment, and repulsive interactions. (E) A representative energy barrier profile for $H = K = R = V = 0$ (dashed curves). The energy profile for $H, K, R, V \neq 0$ for a transition between the states considered in (D) is shown by the thick solid curve.

force along the pore (resulting from interactions of the different species with the constituents of the pore interior) are embodied by site-dependent transition rates p_{\pm} and k_{\pm} . Thus, MD-derived potentials of mean force used in previous models can also be implemented within our lattice framework. Such effects of local inhomogeneities in the hopping rates have been studied analytically and with MC simulations in related models [Kolomeisky 1998].

The basic model described above has been studied analytically in certain limits where exact asymptotic results for the steady-state proton current J were derived [Chou 2002]. However, this study did not explicitly include any interactions other than proton exclusion and proton transfer onto properly aligned water dipoles. Effects arising from forces such as repulsion between protons in close proximity, interactions between water dipoles and external electric fields, and dipolar coupling between neighboring waters need to be considered.

In Fig 3A, a proton moves down the electric potential reducing the total enthalpy by V , and a right-pointing dipole is converted into a left-pointing dipole at an energy cost of H . Since both initial and final states have adjacent, repelling protons, the repulsion energy R does not enter in the overall energy change. In Fig. 3B, a proton moves down the potential ($-V$), a “+” water is converted to a “-”, ($+H$), a dipole “domain wall” is removed ($-K$), and the repulsive energy between adjacent charged protons is relieved ($-R$). The representation of these nearest neighbor effects can be succinctly written in terms of the energy of a specific configuration

$$E[\{\sigma_i\}] = -K \sum_{i=1}^{N-1} \sigma_i \sigma_{i+1} - H \sum_{i=1}^N \sigma_i + R \sum_{i=1}^{N-1} (1 - \sigma_i^2)(1 - \sigma_{i+1}^2) - V \sum_{i=1}^N i(1 - \sigma_i^2). \quad (1)$$

The H, K, R, V parameters used in $E[\{\sigma_i\}]$ are all in units of $k_B T$ and represent

- H : energy cost for orienting a water dipole against external field
- K : energy cost for two oppositely oriented, adjacent dipoles
- R : repulsive Coulombic energy of two adjacent protons
- V : energy for moving a charged proton one lattice site against an external field.

V as the change in potential that a proton incurs as it moves between adjacent waters. The total transmembrane potential $V_{membrane} = NV$. The local dielectric environment across a channel can induce a spatially varying effective potential $V_{1 \leq i \leq N}$ [Edwards *et al.* 2002, Jordan 1984, Partenskii & Jordan 1992, Szygnow & von Kitzing 1999]. In this study, we

neglect this variation and assume constant V across the lattice.

In order to connect the quantities $H, K, R,$ and V to the rates $\alpha, \beta, \gamma, \delta, p_{\pm}, k_{\pm}$, we will assume the transitions occur over thermal barriers. Although barriers to proton hopping may be small, we employ the Arrhenius forms in order to obtain a simple relationship so that qualitative aspects of the effects of $H, K, R,$ and V can be illustrated. Activation-energy-based treatments for conduction across gramicidin channels have been previously studied [Chernyshev & Cukierman 2002]. When the more complicated interactions and external potentials are turned on, the effective transition rates $\xi \equiv \{\alpha, \beta, \gamma, \delta, p_{\pm}, k_{\pm}\}$ on which we base our Metropolis Monte-Carlo become

$$\xi = \xi_0 \exp\left(\frac{\Delta E}{2}\right), \quad (2)$$

where $\xi_0 \equiv \{\alpha_0, \beta_0, \gamma_0, \delta_0, p_0, k_0\}$ are rate prefactors when H, K, R, V and ΔE are zero. In defining Eq. 2, we have assumed that the energy barrier due to the difference $\Delta E = E[\{\sigma'_i\}] - E[\{\sigma_i\}]$ ($\{\sigma'_i\}$ and $\{\sigma_i\}$ are the final and initial state configurations, respectively) is evenly split between the barrier energies in the forward and backward directions. We use the convention that $p_+ = p_- = p_0$ and $k_+ = k_- = k_0$ when $V = 0$ and $H = 0$, respectively. The constraints and the state-dependent transition rates determined by Eqs. 1 and 2 completely define a nonequilibrium dynamical model which we study using MC simulations. Note that in the original model (Fig. 2) we *do not* assume transition barriers, but rather only that the dynamics are Markovian.

We first gained insight into the dynamics by considering numerical solutions to the full Master equation for a short three site ($N = 3$) channel. If we explicitly enumerated all $27 = 3^3$ states of the three site model, the Master equation for the 27 component state vector \vec{P} is

$$\frac{d\vec{P}(t)}{dt} = \mathbf{M}\vec{P}(t), \quad (3)$$

where \mathbf{M} is the transition matrix constructed from the rates ξ . In steady-state, the P_i are solved by inverting \mathbf{M} with the constraint $\sum_{i=1}^{27} P_i = 1$. The steady-state currents are found from the appropriate elements in P_i times the proper rate constants in the model. For example, if the probability that the three-site chain is in the configuration $(+ - 0)$ is denoted P_{12} , then the transition rate to state $P_{13} \equiv (+ - -)$ (corresponding to the ejection of a proton from the last site into the right reservoir) is βe^{V-H-K} and the steady state current $J = \beta \sum_i' P_i$ (where the sum \sum_i' runs over all configurations that contain a proton at the last site), will contain the term $\beta^{V-H-K} P_{12}$.

Monte-Carlo simulations were implemented for relatively small ($N = 10$) systems by randomly choosing a

site, and making an *allowed* transition with the probability $\xi \exp(E_i - E_f)/r_{max}$, where r_{max} is the maximum possible transition rate of the entire system. In the next time step, a particle is again chosen at random and its possible moves are evaluated. The currents were computed after the system reached steady-state by counting the net transfer of protons across all interfaces (which separate adjacent sites and the reservoirs) and dividing by $N + 1$. Physical values of J are recovered by multiplying by r_{max} . Particle occupation statistics within the chain were tracked by using the definitions of $+$, 0 and $-$ particle densities at each site i : $\rho_+(i) = \langle \sigma_i(\sigma_i + 1)/2 \rangle$, $\rho_0(i) = \langle (1 - \sigma_i^2) \rangle$, and $\rho_-(i) = \langle \sigma_i(\sigma_i - 1)/2 \rangle$, respectively. However, for our subsequent discussion, it will suffice to analyze simply the chain-averaged proton concentration $\bar{\sigma}_0 = \sum_{i=1}^N \rho_0(i)$. All MC results were checked and compared with the exact numerical results from the three-site, 27-state master equation.

RESULTS AND DISCUSSION

Here, we present MC simulation results for a lattice of size $N = 10$. The mechanisms responsible for the different qualitative behaviors are revealed and the effects of each interaction term will be systematically analyzed. We explore a range of relative kinetic rates, all nondimensionalized in units of p_0 , the intrinsic proton hopping rate from between adjacent waters. Estimates for p_0 derived from quantum MD simulations are on the order of 1ps^{-1} [Sadeghi & Cheng 1999, Mavri & Berendsen 1995, Mei *et al.* 1998, Schmitt & Voth 1999].

One of the main features we wish to explore is the effect of multiple proton occupancy on current-voltage relationships. To understand what values of transition rates would permit multiple proton occupancy, consider water at $\text{pH}=7$, which has 10^{-7}M proton and hydroxyls. This concentration corresponds to about $60 \text{H}_3\text{O}^+$ and 60OH^- species per cubic micron. Even at $\text{pH} 4$, one would only have $\sim 60,000$ hydroniums per μm^3 , corresponding to a typical distance between hydroniums of $\sim 25\text{nm}$. Since there are only $\sim 10 - 20$ waters within a single-file channel, and at $\text{pH} 4$, only about one in $500,000$ waters are protonated in bulk, multiple protons in a single channel can occur only if protonated species within the channel are highly stabilized by interactions with the chemical subgroups comprising the pore interior. This stabilizing effect is modeled by small escape rates β_0, γ_0 , and assumed to be distributed equally such that p_0 remains constant across all sites within the lattice. Although from a concentration point of view, small entrance rates α_0, δ_0 arise from infrequent protons that wander into the first site of the channel, their exit rates β_0, γ_0 can be suppressed even more by their stabilization once inside the channel. In all of our simulations, we will assume proton stabilization is moderately strong and limit ourselves rates $\beta_0, \gamma_0 < \alpha_0, \delta_0$. The values we use give steady-state proton occupancies across the whole range of values from $\lesssim 1$ to N .

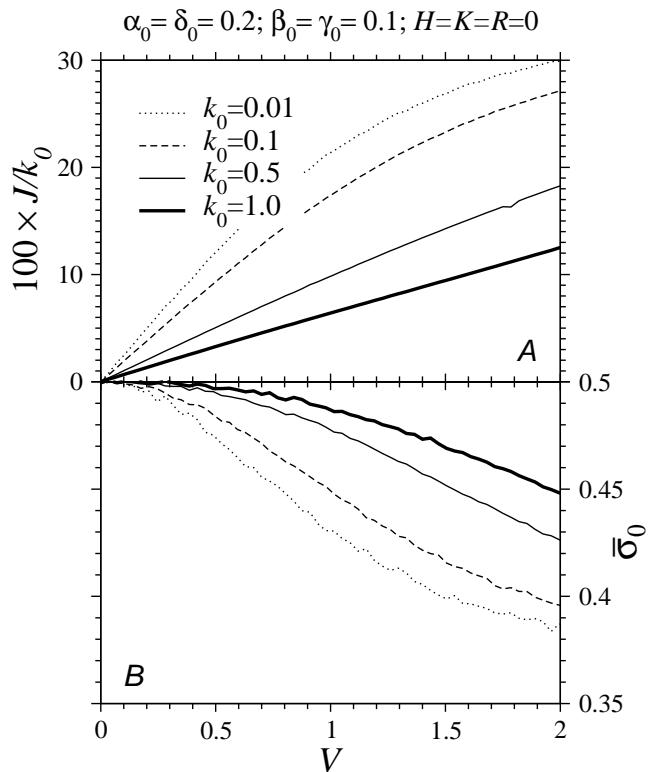


FIG. 4: Saturation due to small flip rates $k_+ = k_- = k_0$. Currents and rates in all plots are nondimensionalized by units of p_0 . (A) Small k_0 determines the rate limiting step whereupon increasing V does little to increase the current. Increasing k_0 pushes the sublinear (saturation) regime of the $J - V$ relationship to larger values of voltage V . (B) The total proton occupancy decreases with decreasing k_0 .

First consider symmetric solutions and featureless, uniform pores where $\alpha_0 = \delta_0, \beta_0 = \gamma_0$. The only possible driving force is an external voltage V . In Fig. 4, we plot the current-voltage relationship for various flipping rates k_0 . We initially ignore interaction effects and set $H = K = R = 0$. Currents for sufficiently small V are always nearly linear. However, for sufficiently large V , the rate limiting step eventually becomes the water flipping rate k_0 . Further increases in V do not increase the overall steady-state current, and the current-voltage curve becomes sublinear before saturating. The crossover to sublinear (water flipping rate limited) behavior depends on the value of k_0 , with sublinear onset occurring at higher voltages V for larger k_0 . In the noninteracting case, for most reasonable values of rate constants, any possible superlinear regime does not arise as it is washed out by the sublinear, water flip rate-limited saturation. The only instance found where noticeable superlinear behavior in the steady-state proton current arises is in the limit of large k_0 and when $\alpha_0, \delta_0, p_0 \ll \beta_0, \gamma_0$. For the parameters explored, the currents J increase with increasing k_0 (Fig. 4A); thus, the mean proton occupancies are *qualitatively* consistent with dynamics limited by internal

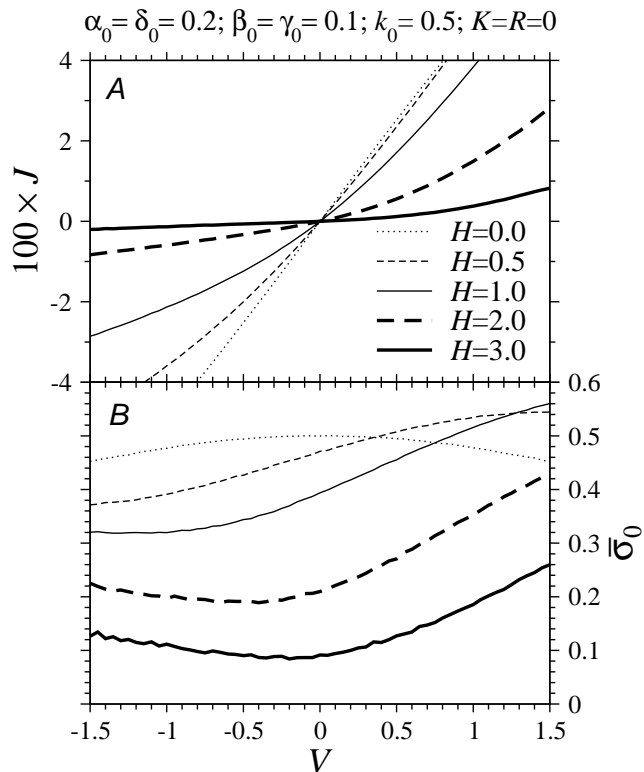


FIG. 5: Currents (A) and averaged proton occupation (B) in the presence of a constant water dipole-aligning field $H > 0$. For larger V , the V -independent H assumption used in this scenario will break down due to the orientation effects of V on the water dipoles.

proton hops. For small flipping rates, successive entry of protons is slow, while exit is not affected. As k_0 is increased, the bottlenecks near the entrance are relieved to a greater degree than those near the exit, increasing the overall proton occupancy (cf. Fig. 4B).

Figure 5 displays the effects of a fixed, external, dipole-orienting field $H \neq 0$. All other interactions and fields, except the external driving voltage V , are turned off. The convention used in the energy Eq. 1 favors a “+” state for $H > 0$. This asymmetry leads to an asymmetry in the $J - V$ relationship (Fig. 5A). After an initial proton has traversed the channel, flipping of the “-” waters left in its wake is suppressed for $H > 0$, thereby preventing further net proton movement. The persistent blockade induced by increasing H is evident in Fig. 5B where the proton density decreases for increasing H .

Although H is held fixed in Fig. 5, physically, dipole alignment fields arise from external electric fields that couple to the permanent dipoles of water. Therefore, we expect that $H = L_{HV}V$ where L_{HV} represents the orientational polarizability of the water molecule. It has been conjectured that when L_{HV} is positive (defined as preferring waters with lone pairs pointing to the left, or in the “+” state), the current should increase superlinearly with V since waters ahead of any proton will be oriented prop-

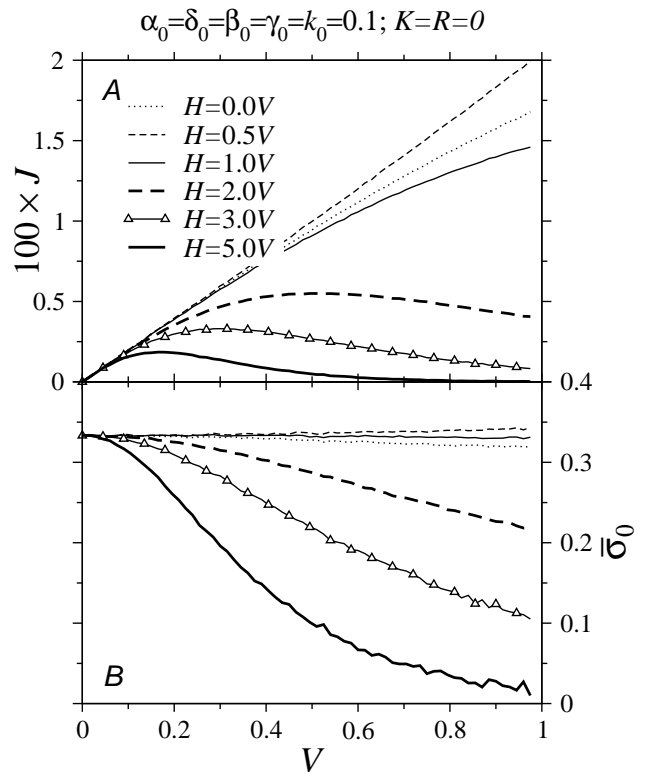


FIG. 6: (A) Negative differential resistance (NDR) for large L_{HV}, V . Although transitions such as $\dots - +0 - + \dots \rightarrow \dots - +0 + + \dots$ are accelerated, giving rise to a state where proton transport to the right is possible, NDR can arise because transitions such as $\dots - +0 + + \dots \rightarrow \dots - + - 0 + \dots$ created an additional “-” particle and is disfavored. (B) The average proton occupation *decreases* as V for large L_{HV} .

erly as to receive it. Figure 6 shows the current-voltage relationship for various L_{HV} . Although for very small L_{HV} , the current does increase very slightly, it becomes severely sublinear for larger L_{HV} and V . In fact, it can attain a negative differential resistance (NDR) similar to that found in Gunn diodes or other “negistor” devices. The physical origins of NDR in proton conduction arise from the energetic cost of producing a “-” state as a proton moves forward. Although the path ahead of the proton is biased to “+” states, the proton transfer step as defined in our model *necessarily* leaves behind a “-” particle. Thus, although the field $H = L_{HV}V$ properly aligns waters ahead of a proton, it also provides an energy cost for the tail of “-” particles left by a forward-moving proton. This energetic penalty inhibits the proton from moving forward despite the direct driving force V acting on it.

The average density plotted in Fig. 6B decreases as V or large L_{HV} . Large L_{HV} not only hinders forward proton hops, but enhances backward hops of protons that have just hopped forward during its previous time step. Proton dynamics are slowed dramatically, and only at the last site can they exit the pore. Proton entry from

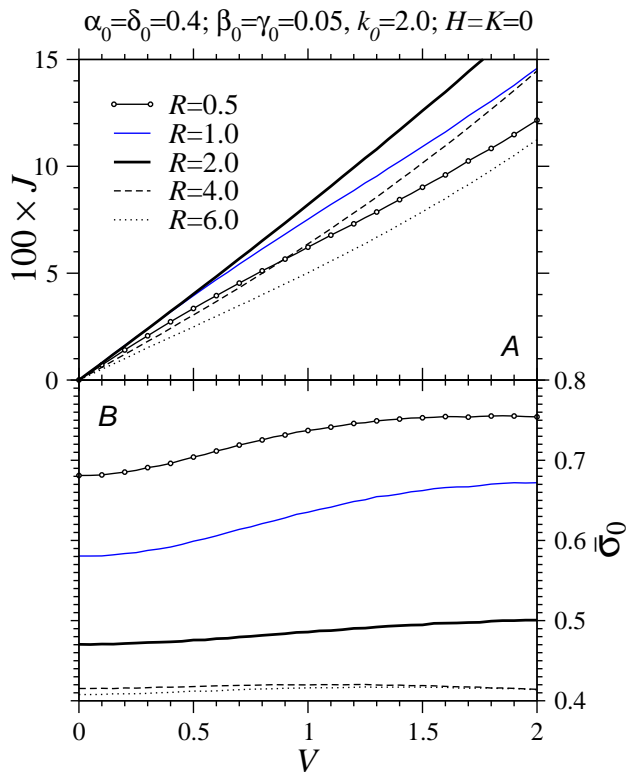


FIG. 7: The effects of increasing nearest-neighbor proton-proton repulsion within the chain. Fixed parameters are $\alpha_0 = \delta_0 = 0.4$, $\beta_0 = \gamma_0 = 0.05$, $k_0 = 2.0$, and $H = K = 0$. (A) The onset of sublinear behavior in the $J - V$ relationship is delayed for larger repulsions R , making the curves appear locally more superlinear. (B) The average proton densities per site. For small R , although densities are high, increasing V increases the clearance rate near the entrance such that the effectively increased injection increases overall proton density. At higher repulsions R , the clearance effects is not as strong and the simultaneously increased extraction rate prevents a large increase in the overall proton density.

the left reservoir on the other hand, is often quickly followed by exit back into the left reservoir. The protons are *effectively* entry-limited, and the density is rather low. As V increases, the dynamics become even more “entry-limited,” and the overall proton occupancy decreases.

The effects of proton-proton repulsion ($R > 0$) are considered in Figs 7 and 8. These simulations are consistent with the hypothesis that proton-proton repulsions can give rise to superlinear current [Hille & Schwarz 1978]. Figure 7A shows a slight preference for superlinear behavior as repulsion R is increased. Not surprisingly, Fig. 7B shows that the overall density of protons within the pore decreases with increasing repulsion.

The sublinear-to-superlinear behavior as the proton concentration in the identical reservoirs is increased is shown in Fig. 8A. Although for these parameters, the effect is not striking, there is indeed a trend away from sublinear behavior as pH is decreased, or, as $\alpha_0 = \delta_0$ is increased. Mea-

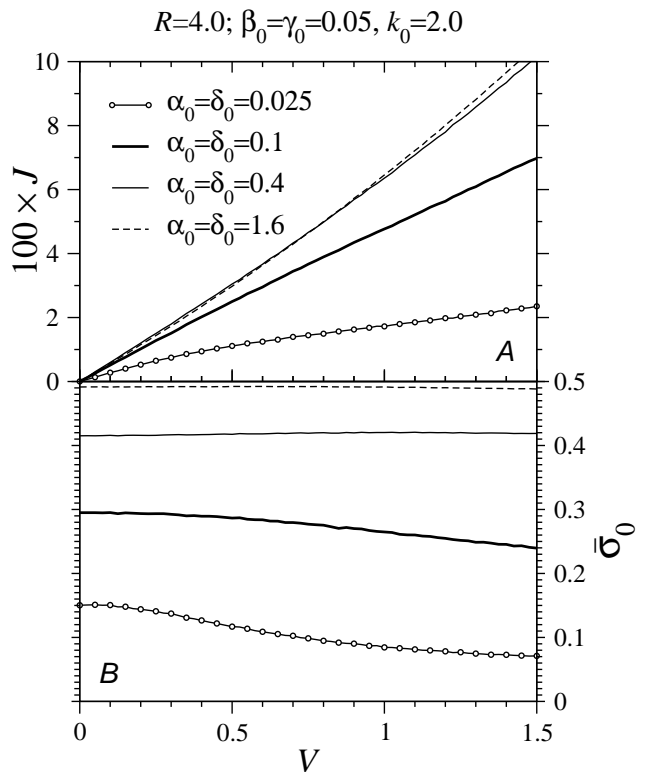


FIG. 8: Transition from sublinear to superlinear current behavior as proton concentration in the symmetric reservoirs is increased. (A) $J - V$ relationship for various concentrations $\alpha_0 = \delta_0$ for fixed $H = K = 0$, $R = 4.0$, $\beta_0 = \gamma_0 = 0.05$, and $k_0 = 2.0$. (B) The averaged proton concentration σ_0 at each lattice site as a function of driving voltage. The concentrations increase for all ranges of V as $\alpha = \delta$ is increased.

surements, though, also show rather modest superlinear behavior [Eisenman *et al.* 1980, Phillips *et al.* 1999, Rokitskaya *et al.* 2002]. The occupancy also increases with decreasing pH, enhancing the effect of proton-proton repulsion. These behaviors are consistent with experimental findings [Eisenman *et al.* 1980] and those in the simulations depicted in Fig. 7 where increased repulsion exhibited superlinear $J - V$ curves.

Finally, we consider the effects of dipole coupling $K \neq 0$ between adjacent water molecules. This interaction is analogous to a nearest neighbor ferromagnetic coupling in *e.g.*, Ising models. Fig. 9A shows that for sufficiently large $\alpha_0 = \delta_0$, a superlinear behavior arises (for small enough V and large enough k_0 such that saturation has not yet occurred). Notice that as $\alpha_0 = \delta_0$ is increased, the $J - V$ relationship can become more sublinear before turning superlinear. Here, we have used a higher value of k_0 to suppress sublinear behavior to larger V , but the qualitative shift from sublinear to slightly superlinear behavior exists for small k_0 . Moreover, recent comparisons between gramicidin A and gramicidin M channels suggest that water reorientation is not rate-limiting [Gowen *et al.* 2002]. The nature of the superlinear be-

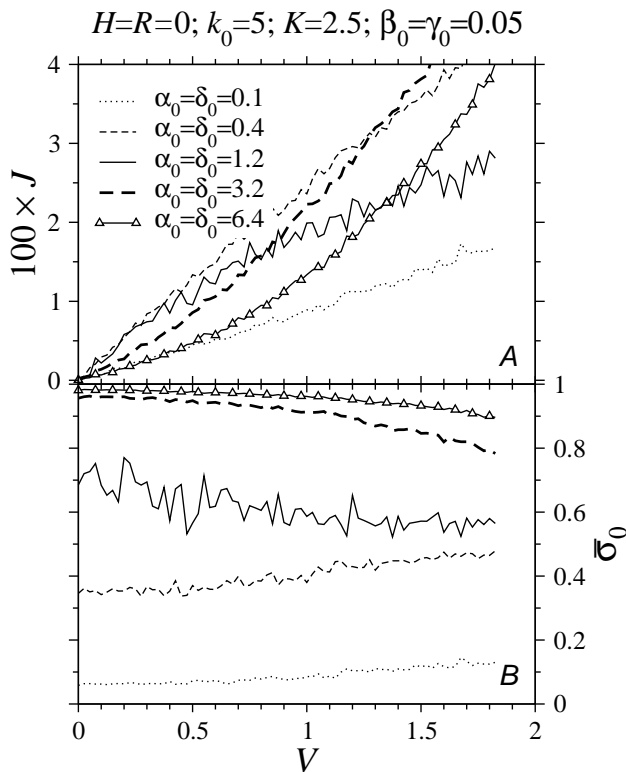


FIG. 9: (A) The current-voltage relationship for various proton injection rates in the presence of ferromagnetic water dipole coupling. (B) Mean proton occupations increase with increasing injection rates.

havior can be deduced from Fig. 9B, where the mean proton density is shown to increase with $\alpha_0 = \delta_0$. Waters that neighbor a proton are relieved of their dipolar coupling and can more readily flip to a configuration that would allow acceptance of another proton. For example, the transition $\dots 0-0\dots \rightarrow \dots 0+0\dots$ will occur faster than $\dots -0\dots \rightarrow \dots -+0\dots$. This lubrication effect arises only when the proton density is high and $K \neq 0$.

SUMMARY AND CONCLUSIONS

We have developed a lattice model for proton conduction that quantifies the kinetics among three approximate states of the individual water molecules inside a simple, single-file channel such as gramicidin A. The three states represent water molecules with left and right-pointing water dipoles, and protonated ions. Our approach allows us to explore the *steady-state* behavior of proton currents, occurring over timescales inaccessible by MD simulations. The model, along with analyses of Monte-Carlo simulations, also extends analytic models [Schumaker *et al.* 2000, Schumaker *et al.* 2001] to include multiple proton occupancy and the memory effects of protons that have recently traversed the water-wire. Monte-Carlo simulations of the lattice model was performed to test conjectures on a number of observed qualitative features in proton transport across water wires.

Four interaction energies that modify the kinetic rates are considered: A dipole-orienting field which tends to align the water molecules, a ferromagnetic dipole-dipole interaction terms between neighboring water molecules, a penalty from the repulsion between neighboring protons, and an external electric field (transmembrane potential) that biases the hops of the charged protons.

We find current-voltage relationships that can be both superlinear and sublinear depending on the voltage V . For large enough voltages, the proton hopping step is no longer rate limiting. Water flipping rates limit proton transfer and further increases in V do little to increase the steady-state proton current J . This observation suggests that the observed transition from sublinear to superlinear behavior can be effected by varying an *effective* water flipping rate. Although we find that indeed proton-proton repulsion can lead to slightly superlinear $J - V$ characteristics, particularly for large repulsions and proton injection rates (low pH).

Dipole-dipole interactions between neighboring waters are also incorporated. Previous single-proton theories [Schumaker *et al.* 2000, Schumaker *et al.* 2001] have considered the propagation of a single defect back and forth in the pore. In our model, the number of protons and defects are dynamical variables that depend on the injection rates and the dipole-dipole coupling, respectively. For large coupling K , we expect very few defects, and effective water flipping rates will be low. However, when injection rates and proton occupancy in the pore is high, some dipole-dipole couplings are broken up by the intervening protons. Thus, protons can “lubricate” their neighboring dipoles, allowing them to flip faster than if they were neighboring a dipole pointed in the same direction. Using simulations, we showed that this lubrication effect can give rise to a superlinear $J - V$ relationship

Although the parameters used in our analyses can be further refined by estimating them from shorter time MD simulations, or other continuum approaches [Edwards *et al.* 2002, Partenskii & Jordan 1992]. More complicated local interactions with membrane lipid dipoles [Rokitskaya *et al.* 2002] and internal pore constituents (such as Trp side groups [Dorigo *et al.* 1999, Gowen *et al.* 2002]) can be incorporated by allowing H, K, p_0 and/or k_0 to reflect the local molecular environment by varying along the lattice site (position) within the channel [Kolomeisky 1998].

The author thanks Mark Schumaker for vital discussions and comments on the manuscript. This work was performed with the support of the National Science Foundation through grant DMS-0206733, and the National Institutes of Health through grant R01 AI41935.

APPENDIX A: NOINTERACTING MEAN-FIELD RESULTS

For the sake of completeness, and as a guide to aid qualitative understanding, we review analytic results in the case $R = K = H = 0$, where only exclusions are included. Some of these results have been derived previously using mean-field approximations [Chou 2002].

If $V = 0$ ($\xi = \xi_0$), only pH differences between the two reservoirs can affect a nonzero steady-state proton current. The proton concentration difference is reflected by a difference between the entry rates from the two reservoirs $\alpha_0 \neq \delta_0$, and the steady-state current can be expanded in powers of $1/N$: $J = a_1/N + a_2/N^2 + \mathcal{O}(N^{-3})$. In the long chain limit, we found [Chou 2002]

$$J \sim \frac{k_+ k_-}{N(k_+ + k_-)} \times \ln \left[\frac{\beta(k_+ + k_-) + k_+ \delta}{\gamma(k_- + k_+) + k_- \alpha} \frac{\gamma(k_+ + k_-) + \alpha(p_- + k_-)}{\beta(k_+ + k_-) + k_+ \delta(p_- / k_- + 1)} \right] + \mathcal{O}(N^{-2}). \quad (\text{A1})$$

For channels with reflection-symmetric molecular structures, $\beta_0 = \gamma_0$, and Eq. A1 can be further simplified by expanding in powers of $k_- \alpha - k_+ \delta$,

$$J \sim \frac{\beta p_+ k_- (k_- \alpha - k_+ \delta)}{N [\beta(k_- + k_+) + k_+ \delta] (\beta + \delta) (k_+ + k_-)} + \mathcal{O}((k_- \alpha - k_+ \delta)^2) + \mathcal{O}(1/N^2), \quad (\text{A2})$$

Finally, in the *large* α and $\delta = 0$ limit,

$$J \sim \frac{k_+ k_-}{(k_+ + k_-) N} \log \left(1 + \frac{p_-}{k_+} \right) - \frac{\gamma k_+ k_- p_-}{\alpha N (k_+ + k_-) (k_+ + p_-)} + \mathcal{O}(\alpha^{-2} N^{-1}). \quad (\text{A3})$$

For driven systems, where, say, $\alpha > \delta, \beta > \gamma$, and $p_+ > p_-$, a finite current persists in the $N \rightarrow \infty$ limit. We can use mean-field approximations familiar in the totally asymmetric simple exclusion process (TASEP) [Derrida 1998, Schutz & Domany 1993] to conjecture that three current regimes exist. If the both proton entry and exit is fast, and the rate-limiting steps involve water flipping, or interior protons hops with rate p_+ , we expect that a maximal current regime exists and that the densities of the three states along the interior of a long chain are spatially uniform. Mean-field analysis from previous work [Chou 2002] yields

$$J = \frac{2(p_+ k_- - p_- k_+)}{(p_+ + p_-)^2} \left[\frac{(p_- + p_+)}{2} + k_- + k_+ - \sqrt{k_+ + k_-} \sqrt{k_- + k_+ + p_+ + p_-} \right]. \quad (\text{A4})$$

For a purely asymmetric process, $p_- = 0$, and the current approaches the analogous maximal-current expression of the single species TASEP,

$$J(p_- = 0) \sim \frac{p_+ k_-}{4(k_- + k_+)} + \mathcal{O}\left(\frac{p_+}{k_-}\right), \quad (\text{A5})$$

except for the additional factor of $k_-/(k_- + k_+)$ representing the approximate fraction of time sites ahead of a proton are in the $+$ configuration. These approximations neglect the influence of protons that have recently passed, temporarily biasing the water to be in a “ $-$ ” configuration. Therefore, it is not surprising that these results are accurate only in the $k_+, k_- \gg p$ limit.

A similar approach is taken when the currents are entry or exit limited. From the mean-field approximation of the steady-state equation for ρ_{\pm} near the channel entry,

$$\begin{aligned} \frac{\partial \rho_-}{\partial t} &= p_+ \rho_0 \rho_+ + k_+ \rho_+ - k_- \rho_- = 0 \\ \frac{\partial \rho_+}{\partial t} &= -\alpha \rho_+ - k_+ \rho_+ + k_- \rho_- = 0, \end{aligned} \quad (\text{A6})$$

where we have for simplicity set $p_- = \gamma = 0$. Upon using normalization $\rho_- + \rho_0 + \rho_+ = 1$, and Eqs. A6, we find the mean densities near the left boundary

$$\begin{aligned} \rho_- &= \frac{(\alpha + k_-)(p_+ - \alpha)}{p_+(\alpha + k_- + k_+)}, \\ \rho_+ &= \frac{k_-(p_+ - \alpha)}{p_+(\alpha + k_- + k_+)}, \end{aligned} \quad (\text{A7})$$

and the approximate entry rate-limited steady-state current

$$J \approx p_+ \rho_0 \rho_+ = \alpha \rho_+ = \frac{\alpha k_- (1 - \alpha/p)}{(\alpha + k_- + k_+)}. \quad (\text{A8})$$

This result resembles the steady-state current of the low density phase in the simple exclusion process [Derrida 1998, Chou 2003], except for the factor $k_-/(\alpha + k_- + k_+)$ representing the fraction of time the first site is in the $+$ state, and able to accept a proton from the left reservoir.

When the rate β is rate-limiting, we consider the mean-field equations near the exit of the channel

$$\begin{aligned} \frac{\partial \rho_-}{\partial t} &= \beta \rho_0 + k_+ \rho_+ - k_- \rho_- = 0 \\ \frac{\partial \rho_+}{\partial t} &= -p_+ \rho_0 \rho_+ + k_- \rho_- - k_+ \rho_+ = 0, \end{aligned} \quad (\text{A9})$$

and their solutions

$$\rho_- = \frac{\beta(k_+ + p_+ - \beta)}{p_+(k_- + \beta)}, \quad \rho_+ = \frac{\beta}{p_+}. \quad (\text{A10})$$

The exit-limited steady-state current is thus

$$J \approx \beta\rho_0 = \frac{\beta}{k_- + \beta} \left(k_- - \frac{\beta(k_- + k_+)}{p_+} \right). \quad (\text{A11})$$

The results above are derived from mean-field assumptions which neglect correlations in particle occupancy between neighboring sites. Although mean-field theory

happens to give exact results for the simple exclusion process, the results above are only exact in the large k_{\pm}/p_{\pm} limit, as has been shown by Monte-Carlo simulations [Chou 2002]. Only in this limit, where the memory of a previously passing proton is quickly erased, are the mean-field results quantitatively accurate [Chou 2002]. Nonetheless, the mean-field calculations of the simplified system ($H = K = R = 0$) yields qualitatively correct results for the steady-state current, provides a connection with well-known results of the TASEP, and gives an explicit qualitative description of the mechanisms at play.

Agmon, N. 1995. The Grotthuss mechanism. *Chem. Phys. Lett.* 244:456-462.

B. Alberts, D. Bray, J. Lewis, M. Raff, K. Roberts and J. D. Watson, *Molecular biology of the cell*, (Garland Publishing, New York, 1994).

Akeson, M., and D. W. Deamer. 1991. Proton conductance by the gramicidin water wire: Model for proton conductance in the F1F0 ATPases? *Biophys. J.*, 60:101-109.

Andersen, O. S. 1983. Ion movement through gramicidin A channels. Single-channel measurements at very high potentials. *Biophys. J.*, 41:119-133.

Bala, P., B. Lesyng, and J. A. McCammon. 1994. Applications of quantum-classical and quantum-stochastic molecular dynamics for proton transfer processes. *Chem. Phys.* 180:271-285.

Boyer, P. 1997. The ATP synthase - a splendid molecular machine. *Annu. Rev. Biochem.* 66:717-749.

Busath, D. D., C. D. Thulin, R. W. Hendershot, L. R. Phillips, P. Maughn, C. D. Cole, N. C. Bingham, S. Morrison, L. C. Baird, R. J. Hendershot, M. Cotten, and T. A. Cross. 1998. Non-contact dipole effects on channel permeation. I. Experiments with (5F-indole)Trp-13 gramicidin A channels. *Biophys. J.* 75:2830-2844.

Chernyshev, A. and S. Cukierman. 2002. Thermodynamic View of Activation Energies of Proton Transfer in Various Gramicidin A Channels. *Biophys. J.* 82:182-192.

Chou, T. 1998. How Fast do Fluids Squeeze Through Microscopic Single-File Channels? *Phys. Rev. Lett.* 80:85-89.

Chou, T. 1999. Kinetics and thermodynamics across single-file pores: solute permeability and rectified osmosis. *J. Chem. Phys.* 110:606-615.

Chou, T. and D. Lohse. 1999. Entropy-driven pumping in zeolites and ion channels. *Phys. Rev. Lett.* 82:3552-3555.

Chou, T. 2002. A spin flip model for one-dimensional water wire proton transport. *J. Phys. A.* 35:4515-4526.

Chou, T. 2003. Ribosome recycling, diffusion, and mRNA loop formation in translational regulation. *Biophys. J.* 85:755-773.

Cotten, M., C. Tian, D. D. Busath, R. B. Shirts, and T. A. Cross. 1999. Modulating dipoles for structure-function correlations in the gramicidin A channel. *Biochemistry.* 38:9185-9197.

Cukierman, S., E. P. Quigley, and D. S. Crumrine. 1997. Proton conductance in gramicidin A and its dioxolane-linked dimer in different bilayers. *Biophys. J.* 73:2489-2502.

Deamer, D. W. 1987. Proton permeation of lipid bilayers. *J. Bioenerg. Biomembr.* 19:457-479.

Dcornez, H., K. Drukker, and S. Hammes-Schiffer. 1999. Solvation and hydrogen-bonding effects on proton wires. *J. Phys. Chem. A.* 103:2891-2898.

Derrida, B. 1998. An exactly soluble non-equilibrium system: The asymmetric simple exclusion process. *Physics Reports* 301:65-83.

DeCoursey, T. E., and V. V. Cherny. 1994. Voltage-activated hydrogen ion currents. *J. Membr. Biol.* 141:203-223.

Dorigo, A. E., D. G. Anderson, and D. D. Busath. 1999. Non-contact dipole effects on channel permeation. II. Trp conformations and dipole potentials in gramicidin A. *Biophys. J.* 76:1897-1908.

Edwards, S., B. Corry, S. Kuyucak, and S.-H. Chung. 2002. Continuum Electrostatics Fails to Describe Ion Permeation in the Gramicidin Channel. *Biophys. J.* 83: 1348 - 1360.

Eisenman, G., B. Enos, J. Hägglund, and J. Sandblom. 1980. Gramicidin as an example of a single-filing ionic channel. *Ann. N.Y. Acad. Sci.* 339:8-20.

Fisher, M. E., and A. B. Kolomeisky. 1999. The force exerted by a molecular motor. *Proc. Natl Acad. Sci. USA.* 96:6597-6602.

Grabe, M. and G. Oster. 2001. Regulation of Organelle Acidity. *J. Gen. Physiol.* 117:329-343.

Gowen, J. A., J. C. Markham, S. E. Morrison, T. A. Cross, D. A. Busath, E. J. Mapes, and M. F. Schumaker. 2002. The Role of Trp Side Chains in Tuning Single Proton Conduction through Gramicidin Channels. *Biophys. J.* 83:880-898.

Grotthuss, C. J. T. 1806. Sur la décomposition de l'eau et des corps qu'elle tient en dissolution à l'aide de l'électricité galvanique, *Ann. Chim.* 58:54-74.

Hille, B., and W. Schwarz. 1978. Potassium channels as multi-ion single-file pores. *J. Gen. Physiol.* 72:409-442.

- Hladky, S. B., and D. A. Haydon. 1972. Ion transfer across lipid membranes in the presence of gramicidin A. I. Studies of the unit conductance channel. *Biochim. Biophys. Acta.* 274:294-312.
- Hu, W., and T. A. Cross. 1995. Tryptophan hydrogen bonding and electrical dipole moments: functional roles in the gramicidin channel and implications for membrane proteins. *Biochemistry.* 34:14147-14155.
- Hummer, G., J. C. Rasaiah, and J. P. Noworyta. 2001. Water conduction through the hydrophobic channel of a carbon nanotube. *Nature* 414:188-190.
- Jordan, P. C. 1984. The total electrostatic potential in a gramicidin channel. *J. Membr. Biol.* 78:91-102.
- Kalra, A., S. Garde, and G. Hummer. 2003. Osmotic water transport through carbon nanotube membranes. *Proc. Natl. Acad. Sci. USA* 100:10175-10180.
- Karimipour, V. 1999. Multispecies asymmetric simple exclusion process and its relation to traffic flow *Phys. Rev. E* 59:205-212.
- Kolomeisky, A.B. 1998. Asymmetric simple exclusion model with local inhomogeneity. *J. Phys. A: Math. Gen.* 31:1153-1164.
- Lanyi, J. K. 1995. Bacteriorhodopsin as a model for proton pumps. *Nature.* 375:461-463.
- Levitt, D. G., S. R. Elias, and J. M. Hautman. 1978. Number of water molecules coupled to the transport of sodium, potassium and hydrogen ions via gramicidin, nonactin or valinomycin. *Biochim. Biophys. Acta.* 512:436-451.
- Lynden-Bell, R. M., and J. C. Rasaiah. 1996. Mobility and solvation of ions in channels. *J. Chem. Phys.* 105:9266-9280.
- MacDonald, C. T. and J. H. Gibbs. 1969. Concerning the Kinetics of Polypeptide Synthesis on Polyribosomes. *Biopolymers*, 7:707-725.
- Marx, D., M. E. Tuckerman, J. Hutter, and M. Parrinello. 1999. The nature of the hydrated excess proton in water. *Nature.* 397:601-604.
- Mavri, J., and H. J. C. Berendsen. 1995. Calculation of the proton transfer rate using density matrix evolution and molecular dynamics simulations: inclusion of the proton excited states. *J. Phys. Chem.* 99:12711-12717.
- Mei, H. S., M. E. Tuckerman, D. E. Sagnell, and M. L. Klein. 1998. Quantum nuclear ab initio molecular dynamics study of water wires. *J. Phys. Chem. B.* 102:10446-10458.
- Nagle, J. F. 1987. Theory of passive proton conductance in lipid bilayers. *J. Bioenerg. Biomembr.* 19:413-426.
- Nagle, J. F., and H. J. Morowitz. 1978. Molecular mechanisms for proton transport in membranes. *Proc. Natl. Acad. Sci. USA.* 75:298-302.
- Nagle, J. F., and S. Tristram-Nagle. 1983. Hydrogen bonded chain mechanisms for proton conduction and proton pumping. *J. Membr. Biol.* 74:1-14.
- Partenskii, M. B., and P. C Jordan. 1992. Nonlinear dielectric behavior of water in transmembrane ion channels: ion energy barriers and the channel dielectric constant. *J. Chem. Phys.* 96:3906-3910.
- Phillips, L. R., C. D. Cole, R. J. Hendershot, M. Cotten, T. A. Cross, and D. D. Busath. 1999. Noncontact Dipole Effects on Channel Permeation. III. Anomalous Proton Conductance Effects in Gramicidin. *Biophys. J.* 77:2492-2501.
- Pomès, R., and B. Roux. 1996. Structure and dynamics of a proton wire: A theoretical study of H⁺ translocation along the single-file water chain in the gramicidin A channel. *Biophys. J.* 71:19-39
- Pomès, R., and B. Roux. 1998. Free energy profiles for H⁺ conduction along hydrogen-bonded chains of water molecules. *Biophys. J.* 75:33-40.
- Prokop, P., and L. Skála. 1994. Theory of proton transport along a hydrogen bond chain in an external field. *Chem. Phys. Lett.* 223:279-282.
- Rokitskaya, T. I., E. A. Kotova, and Y. N. Antonenko. 2002. Membrane Dipole Potential Modulates Proton Conductance through Gramicidin Channel: Movement of Negative Ionic Defects inside the Channel. *Biophys. J.* 82:865-873.
- R. R. Sadeghi and H.-P. Cheng. 1999. The dynamics of proton transfer in a water chain. *J. Chem. Phys.* 111:2086-2094.
- Sagnella, D. E., K. Laasonen, and M. L. Klein. 1996. Ab initio molecular dynamics study of proton transfer in a polyglycine analog of the ion channel gramicidin A. *Biophys. J.* 71:1172-1178.
- Sagnella, D. E., and G. A. Voth. 1996. Structure and dynamics of hydronium in the ion channel gramicidin A. *Biophys. J.* 70:2043-2051
- Scheiner, S. 1985. Theoretical studies of proton transfers. *Acc. Chem. Res.* 18:174-180.
- Schmitt, U. W., and G. A. Voth. 1999. The computer simulation of proton transport in water. *J. Chem. Phys.* 111:9361-9381.
- Schreckenber, M., A. Schadschneider, K. Nagel, and N. Ito. 1995. *Phys. Rev. E* 51:2939-2949.
- Schumaker, M. F., R. Pomès, and B. Roux. 2000. A Combined Molecular Dynamics and Diffusion Model of Single-Proton Conduction through Gramicidin. *Biophys. J.* 78:2840-2857.
- Schumaker, M. F. and R. Pomès, and B. Roux. 2001. Framework Model For Single Proton Conduction through Gramicidin, *Biophys. J.* 80:12-30.
- Schütz, G. and E. Domany. 1993. Phase Transitions in an Exactly Soluble One-Dimensional Exclusion Process. *J. Stat. Phys.* 72:277-296.
- A. Syganow and E. von Kitzing. 1999. (In)validity of the Constant Field and Constant Currents Assumptions in Theories of Ion Transport. *Biophys. J.* 76:768-781.
- Wu, Y., and G. A. Voth. 2003. A Computer Simulation Study of the Hydrated Proton in a Synthetic Proton Channel. *Biophys. J.* 85:864-875.